**Title**

# zGrad: A nanobody-based degron system to inactivate proteins in zebrafish.

Naoya Yamaguchi[1], Tugba Colak-Champollion[1] and Holger Knaut[1]

1) Skirball Institute of Biomolecular Medicine, New York University School of Medicine, 540 First Avenue, New York, NY 10016, USA

**Abstract**

The analysis of protein function is essential to modern biology. While protein function has mostly been studied through gene or RNA interference, more recent approaches to degrade proteins directly have been developed. Here, we adapted the anti-GFP nanobody-based system deGradFP from flies to zebrafish. We named this system zGrad and show that zGrad efficiently degrades transmembrane, cytosolic and nuclear GFP-tagged proteins in zebrafish in an inducible and reversible manner. Using tissue-specific and inducible promoters in combination with functional GFP-fusion proteins, we demonstrate that zGrad can inactivate transmembrane, cytosolic and nuclear proteins globally, locally and temporally with different consequences. Global protein depletion results in phenotypes similar to loss of gene activity while local and temporal protein inactivation yields more restricted and novel phenotypes. Thus, zGrad is a versatile tool to study the spatial and temporal requirement of proteins in zebrafish.

## Introduction

The study of the consequences of the loss of gene function is a central technique in biology. In principle, loss of gene function can be achieved through gene, mRNA or protein inactivation. While there are many techniques available to inactivate genes and mRNA globally, spatially and temporally (1), methods to reduce protein function in the same manners are more limited. One strategy to inactivate a specific protein is to fuse it to a degron, a protein domain that targets its fusion partner for degradation. Degrons are recognized by adapter proteins. These adapter proteins target the degron together with its fusion partner to the E3 ubiquitin ligase complex for degradation by the proteasome. By manipulating degrons with temperature, light, small molecules or another protein, protein-degron fusions can also be degraded in a controlled manner (2). Different versions of these approaches have been adapted to zebrafish (3-6) but a method to efficiently deplete proteins and compromise their function is currently not available in zebrafish.

GFP-based fluorescent proteins (FPs) are convenient degrons because they are often used to tag proteins and their degradation can be easily monitored by light microscopy. deGradFP, a system developed in flies, depletes FP-tagged proteins (7). It relies on the expression of an anti-GFP nanobody/F-box fusion protein. This fusion protein recruits FP-tagged proteins to the SKP1- CUL1-F-box (SCF) E3 ubiquitin ligase complex, leading to its ubiquitylation and proteasome-mediated degradation in two to three hours. Slight variations of this system have been used to deplete FP-tagged proteins in different tissues in nematodes (8), flies (9) and in zebrafish nuclei (4).

Here, we surveyed different degron systems in zebrafish and identified an anti-GFP nanobody/F-box fusion protein, which we named zGrad, that efficiently degrades FP-tagged proteins in zebrafish. We used this system to show that zGrad depletes FP-tagged proteins

within 30 to 150 minutes depending on the subcellular localization and the nature of the tagged protein. We found that zGrad-mediated protein degradation recapitulates genetic loss-of-function phenotypes and can uncover severe maternal and maternal-zygotic phenotypes. When we induced zGrad from a heat shock-inducible promoter, we found temporal degradation of FP-tagged proteins with acute and reversible loss-of-protein function phenotypes. Lastly, we expressed zGrad from a tissue-specific promoter and found degradation of FP-tagged proteins exposing a phenotype similar to but less severe than the genetic loss-of-function phenotype. These observations indicate that zGrad is a versatile tool to rapidly and reversibly deplete FP-tagged proteins with temporal or spatial control in zebrafish.

## Results

### zGrad efficiently degrades GFP-tagged proteins in zebrafish

To establish a method to reduce the activity of proteins in zebrafish, we tested several degron-based protein degradation systems. First, we tested the auxin-inducible degron (AID) system (10-12). This system uses the plant F box transport inhibitor response 1 (TIR1) protein to recruit proteins tagged with the small AID degron to the SCF E3 ubiquitin ligase complex in an auxin-dependent manner. We co-injected one-cell stage embryos with *sfGFP-mAID* mRNA and varying amounts of *OsTIR1-mCherry* mRNA and treated them for three hours with or without the auxin analog indole-3-acetic acid (IAA). We found that expression of OsTIR1-mCherry induced degradation of sfGFP-mAID in a dose-dependent manner irrespective of IAA (Figure 1 – figure supplements 1A). We also found that 50 pg/embryo or higher concentrations of *OsTIR1-mCherry* mRNA led to deformed and dying embryos (Figure 1 – figure supplements 1B, C). Thus, low levels of OsTIR1 induce degradation of AID-tagged proteins, higher levels of OsTIR1

are toxic and OsTIR degrades AID-tagged proteins in the absence of auxin, suggesting that, in its current form, the AID system is not suitable to degrade proteins in zebrafish.

Second, we tested the ZIF1/ZF1 tag degradation system. This system uses the *C. elegans* SOCS-box adaptor protein ZIF1 which binds to the zinc-finger domain ZF1 to recruits ZF1-containing protein to the ECS (Elongin-C, Cul2, SOCS-box family) E3 ubiquitin ligase complex for proteasomal destruction (13). We co-injected one-cell stage embryos with *sfGFP-ZF1* mRNA, *ZIF1* mRNA and *mScarlet-V5* mRNA and assessed sfGFP-ZF1 degradation 9 hours later at the epiboly stage. The sequences of the ZF1 tag and ZIF1 were codon optimized for zebrafish and mScarlet-V5 served as an internal standard. Using the ratio of sfGFP to mScarlet fluorescence intensity as a measure, we found that the ZIF1/ZF1 tag degradation only reduced the levels of sfGFP-ZF1 by 17% (Figure 1 – figure supplements 2A, B), indicating that the ZIF1/ZF1 tag degradation system does not efficiently degrade ZF1-tagged proteins in zebrafish.

Third, we tested the Ab-SPOP/FP-tag degradation system. This system uses the CULLIN-binding domain from the human SPOP adaptor protein fused to the anti-GFP nanobody vhhGFP4 (4). The Ab-SPOP hybrid adaptor protein targets nuclear but not cytoplasmic FP-tagged proteins for degradation. We co-injected one-cell stage embryos with *sfGFP-ZF1* mRNA, *Ab-SPOP* mRNA or *Abmut-SPOP* mRNA and *mScarlet-V5* mRNA and assessed sfGFP-ZF1 degradation 9 hours later at the epiboly stage. Abmut-SPOP is a negative control and does not bind FPs because the GFP binding domain in the nanobody is deleted. We assessed the degree of GFP degradation as the ratio of sfGFP to mScarlet fluorescence intensity in the cytoplasm and the nucleus. Consistent with the initial description (4), Ab-SPOP efficiently degraded nuclear sfGFP-ZF1 (70% reduction, Figure 1 – figure supplements 3A-C) but not cytoplasmic sfGFP-ZF1 (13% reduction, Figure 1 – figure supplements 3A-C). Abmut-SPOP did not cause any detectable sfGFP-ZF1 degradation (Figure 1 – figure supplements 3A-C). As

reported previously (4), this confirms that the Ab-SPOP/FP-tag degradation system degrades nuclear proteins efficiently but is not suitable for the degradation of non-nuclear proteins in zebrafish.

Fourth, we tested the deGradFP degradation system. This system uses the F-box domain from the Drosophila Slimb adaptor protein fused to the anti-GFP nanobody vhhGFP4 to target FP-tagged proteins for degradation (Figure 1A, B and (7)). We co-injected one-cell stage embryos with *sfGFP-ZF1* mRNA, *deGradFP* mRNA and *mScarlet-V5* mRNA and assessed sfGFP-ZF1 degradation 9 hours later at the epiboly stage. As above, mScarlet-V5 served as an internal standard and GFP degradation was assessed as the ratio of GFP to mScarlet fluorescence intensity. We found that deGradFP reduced sfGFP-ZF1 only slightly (19% reduction, Figure 1C, D). Since the fusion of the anti-GFP nanobody to the Cullin-binding domain from SPOP resulted in efficient albeit only nuclear degradation of GFP, we reasoned that the anti-GFP nanobody recognizes GFP-tagged proteins but that the Slimb F-box domain is not efficiently recruited to the E3 ligase complex in zebrafish. We therefore replaced the Slimb F-box domain in deGradFP with the homologuous F-box domain from zebrafish, reasoning that this should result in more efficient GFP degradation in zebrafish. Based on sequence homology we identified the zebrafish *fbxw11b* gene as the Drosophila *slmb* orthologue. We then replaced the *Drosophila* F-box domain from Slimb in deGradFP with the zebrafish F-box domain from Fbxw11b (Figure 1A, B). We named this hybrid adaptor protein zGrad for zebrafish deGradFP. To test whether zGrad degrades GFP-tagged proteins, we co-injected one-cell stage embryos with *sfGFP-ZF1* mRNA, *zGrad* mRNA and *mScarlet-V5* mRNA and assessed sfGFP-ZF1 degradation 9 hours later at the epiboly stage using the ratio of sfGFP to mScarlet fluorescence intensity. In contrast to deGradFP, which depleted 19% of sfGFP-ZF1, zGrad depleted sfGFP-ZF1 in both the cytoplasm and the nucleus by 89% (Figure 1C, D). This indicates that zGrad efficiently targets

tagged GFP in the cytoplasm for degradation and should be suitable for assessing protein function in zebrafish.

**zGrad degrades nuclear, transmembrane and cytoplasmic FP-tagged proteins**

Next, we asked whether zGrad degrades GFP-tagged proteins in different cellular compartments using a transgenic line that expresses zGrad from a heat shock inducible promoter in the embryo (*hsp70l:zGrad*).

First, we tested whether zGrad degrades the nuclear protein Histone 2A (H2A). We generated *hsp70l:zGrad* embryos that also expressed H2A-EGFP and H2A-mCherry from two identical 69 kb genomic fragments spanning the *cxcr4b* locus (*cxcr4b:H2A-GFP; cxcr4b:H2A-mCherry*). Among other tissues, the *cxcr4b* promoter drives expression in the somites and the posterior lateral line primordium (primordium) (14). Such embryos were heat shocked at 30 hpf for one hour and imaged over 9.5 hours. Compared to control embryos that did not carry the *hsp70l:zGrad* transgene, H2A-EGFP degradation was discernible in zGrad-expressing embryos within two to three hours post heat shock in all tissues that expressed nuclear EGFP from the *cxcr4b* promoter (skin, pronephros, somites, neural tube and primordium, Figure 2A-E, Figure 2 – Video 1). We quantified H2A-EGFP levels in heat-shocked control embryos and heat-shocked *hsp70l:zGrad* embryos using the fluorescence intensity of H2A-mCherry as a reference. Since H2A-mCherry was expressed from the same promoter as H2A-EGFP and since H2A-mCherry is not recognized by the anti-GFP nanobody and should not be subjected to zGrad-mediated protein degradation (7), comparing the ratio of H2A-mCherry expression levels to H2A-EGFP should be a measure of H2A-EGFP in the absence of zGrad-mediated degradation. Further, we normalized the H2A-EGFP-to-H2A-mCherry fluorescence intensity ratios between zGrad-expressing and heat-shocked control embryos. In the somites, the levels of H2A-EGFP was decreased by 87%, while in the primordium, the levels of H2A-EGFP was decreased by 22%

(Figure 2C). The more efficient degradation of H2A-EGFP in the somites than in the primordium is probably due to the lower levels of H2A-EGFP and the lack of H2A-EGFP production in the somites at the time of zGrad induction.

We further characterized the kinetics of zGrad-mediated degradation by determining the time interval between the start of the heat shock to induce zGrad expression and the first observable difference in EGFP/mCherry levels between zGrad-expressing embryos and the control embryos. We termed this time interval as the time for onset of degradation. We also fitted the EGFP/mCherry ratio to a one-phase exponential decay model to extract the half-life of zGrad-mediated degradation. Although this is a simplification because the model does not account for EGFP production – a variable that we cannot easily measure – we expect that it gives a rough estimate for the time it takes to degrade a GFP-tagged protein once zGrad is expressed. The time for onset of degradation and half-life for H2A-EGFP in the somites was 200 min and 156 min, respectively. The time for onset of degradation and the half-life for H2A-EGFP degradation in the primordium was 140 min and 29 min, respectively (Table 2).

Second, we tested whether zGrad degrades the transmembrane protein E-Cadherin (Cdh1). We generated two transgenes that express Cdh1-sfGFP and Cdh1-TagRFP from a 72 kb genomic fragment spanning the *cdh1* locus (*cdh1:cdh1-sfGFP; cdh1:cdh1-TagRFP*). These transgenes recapitulated the endogenous Cdh1 expression pattern and rescued the lethality of *cdh1* mutant embryos (Table 1), indicating that Cdh1-sfGFP and Cdh1-TagRFP are functional. Using these lines, we generated *hsp70l:zGrad*; *cdh1:cdh1-sfGFP; cdh1:cdh1-TagRFP* embryos and *cdh1:cdh1-sfGFP; cdh1:cdh1-TagRFP* control embryos. These embryos were heat shocked at 31 hpf for one hour and imaged the embryos for 4.8 hours. In zGrad-expressing embryos, Cdh1-sfGFP degradation was uniformly detected within 10 min post heat shock in the skin of the embryo (enveloping layer and epidermal basal layer) (Figure 2F-H, Figure 2 – Video 2). As

192 detailed above for the quantification of zGrad-mediated H2A-EGFP degradation, we used the
193 fluorescence intensity of Cdh1-TagRFP as a reference to quantify the reduction of Cdh1-sfGFP.
194 We divided the Cdh1-sfGFP fluorescence intensity by the Cdh1-TagRFP fluorescence intensity
195 and normalized the ratio in the zGrad-expressing embryos to the ratio in the heat-shocked
196 control embryos. This analysis showed that zGrad expression reduced the levels of Cdh1-
197 sfGFP in the primordium by 79 % with a degradation half-life of 24 min (Figure 2H). The time for
198 onset of Cdh1-sfGFP degradation was 75 min (Table 2).
199
200 Third, we tested whether zGrad degrades the cytoplasmic protein αE-Catenin (Ctnna). To
201 address this, we used a gene trap line that expresses αE-Catenin-Citrine (Ctnna-Citrine) from
202 the *ctnna* locus (15, 16). Homozygous *ctnna-Citrine* fish are viable, indicating that Ctnna-Citrine
203 is functional (15). We generated *hsp70l:zGrad*; *ctnna:ctnna-Citrine/+* embryos and *ctnna:ctnna-*
204 *Citrine/+* control embryos and heat shocked these embryos at 31 hpf for one hour and imaged
205 the embryos for 8 hours. In contrast to heat-shocked control embryos, Ctnna-Citrine was
206 degraded in zGrad-expressing embryos (Figure 2I, J). Since Ctnna tagged with a red
207 fluorescent protein is not available, we could not perform a ratiometric analysis and instead
208 quantified the total Ctnna-Citrine fluorescent intensity. This analysis showed that the time for
209 onset of degradation of Ctnna-Citrine was 65 min and that Ctnna-Citrine was degraded by 58%
210 with a half-life of 19 min in zGrad-expressing embryos (Figure 2K, Table 2).
211
212 Finally, we tested whether zGrad degrades EGFP targeted to the secretory pathway by a signal
213 peptide. Using fish that express secreted EGFP and secreted mCherry from a heat shock
214 promoter (*hsp70l:sec-GFP; hsp70:sec-mCherry*), we generated *hsp70l:sec-GFP; hsp70:sec-*
215 *mCherry; hsp70l:zGrad* embryos and *hsp70l:sec-GFP; hsp70:sec-mCherry* control embryos.

Unlike H2A-EGFP, Cdh1-sfGFP and Ctnna-Citrine, expression of zGrad did not degrade secreted GFP (Figure 2 – figure supplement 1A).

Together, these observations indicate that zGrad efficiently targets nuclear, cytoplasmic, and transmembrane proteins tagged with EGFP or Citrine for degradation.

**zGrad-mediated protein degradation results in loss of protein function**

Since zGrad efficiently degrades proteins from different cellular compartments (Figure 2), we asked whether we can use zGrad-mediated protein depletion to replicate known loss of protein function phenotypes and uncover novel ones. We addressed this question in several ways. First, we tested whether zGrad degrades cytoplasmic Ctnna-Citrine to disrupt its function in cell-cell adhesion (17). We injected *zGrad* mRNA or *sfGFP* control mRNA into one-cell stage embryos that were maternal-zygotic Ctnna-Citrine (*MZ ctnna:ctnna-Citrine*, Figure 3A), maternal Ctnna-Citrine (*M ctnna:ctnna-Citrine*, Figure 3D) or zygotic Ctnna-Citrine (*Z ctnna:ctnna-Citrine*, Figure 3G). In *zGrad* mRNA-injected *MZ ctnna-Citrine* and *M ctnna-Citrine* embryos the cells started to become detached and partly shed from the embryo resulting in embryonic lethality around 3 to 5 hpf (Figure 3B, C, E, F, H, I). Control embryos injected with *sfGFP* mRNA developed normally (Figure 3B, C, E, F, H, I). Similarly but delayed by 20 hours, in *zGrad* mRNA-injected *Z ctnna-Citrine* embryos, cells detached from the embryo by 24 hpf and about half of the embryos died (note, half the embryos are zygotically homozygous for *ctnna:ctnna-Citrine* since we crossed *ctnna:ctnna-Citrine*/*ctnna:ctnna-Citrine* males to *ctnna:ctnna-Citrine*/+ females, Figure 3H, I) while control injected embryos were unaffected (Figure 3H, I). The observed phenotype in *Z ctnna-Citrine* embryos injected with *zGrad* mRNA is similar to the defects reported for zygotic *ctnna*-/- embryos (18). Thus, zGrad depletes Ctnna-Citrine to levels too low to sustain cell-cell adhesion and embryonic development. Moreover, it suggests that

maternally supplied Ctnna can sustain cell-cell adhesion and embryonic development for about one day before the embryo requires zygotic Ctnna.

Second, we tested whether zGrad degrades transmembrane Cdh1-sfGFP efficiently enough to disrupt its function (19-21) and uncover late requirements of Cdh1 in cell-cell adhesion. Such an analysis is currently not possible because *cdh1*-/- embryos die during late gastrulation stages (22-24). To address this, we crossed *hsp70l:zGrad; cdh1+/-; cdh1:cdh1-sfGFP* fish to *cdh1+/-* fish and as a control *cdh1+/-; cdh1:cdh1-sfGFP* fish to *cdh1+/-* fish. We separated *cdh1:cdh1-sfGFP* transgenic from *cdh1:cdh1-sfGFP* non-transgenic embryos from both crosses and separately heat-shocked the embryos for one hour at 25 hpf (Figure 4A). In contrast to control embryos which showed no visible defects (Figure 4C, E), we found that 2.4% of the heat-shocked *cdh1:cdh1-sfGFP* embryos shed their skin and rapidly died (Figure 4B, D), consistent with the idea that zGrad-mediated Cdh1-sfGFP degradation disrupts the cell-cell adhesion between the skin cells of the embryos that lack Cdh1 function. While the expected fraction of embryos that should lose Cdh1 activity and display a phenotype is 6.25% (*cdh1*-/-; *hsp70l:zGrad*; *cdh1:cdh1-sfGFP* embryos, Figure 4 – figure supplement 1A), we believe that not all embryos had enough Cdh1 protein depleted to cause a cell-cell adhesion defect due to the variability in zGrad levels. These observations suggest that transient expression of zGrad can efficiently degrade GFP-tagged proteins and, if GFP-tagged proteins are depleted sufficiently, cause loss of protein function and uncover phenotypes past the initial requirements of essential proteins.

Third, we asked whether induction of zGrad can degrade the Sdf1 chemokine receptor Cxcr4b tagged with EGFP to temporarily disrupt its function as a guidance receptor for the migration of the primordium (25, 26). For this, we heat shocked *hsp70l:zGrad*; *cxcr4b*-/-; *cxcr4b:cxcr4b-EGFP-IRES-Kate2-CaaX-p7* embryos and *cxcr4b*-/-; *cxcr4b:cxcr4b-EGFP-IRES-Kate2-CaaX-p7*

control embryos at 28 hpf when the primordium has completed a third of its migration along the body of the embryo and recorded the levels of Cxcr4b-EGFP and the migration of the primordium by time lapse microscopy. Cxcr4b-EGFP expressed from the *cxcr4b:cxcr4b-EGFP-IRES-Kate2-CaaX-p7* transgene restores the migration of the primordium in *cxcr4b*-/- embryos and Kate2-CaaX expressed from an internal ribosomal entry site (IRES) serves as a marker for the primordium and an internal reference for how much Cxcr4b-EGFP is produced (27, 28). This analysis showed that induction of zGrad degraded Cxcr4b-EGFP (Figure 5A, B, E) and resulted in rounded primordium morphology (Figure 5A, C) and stalled primordium migration (Figure 5A, D, E) 90 min after heat shock. After 120 min newly produced Cxcr4b-EGFP was detectable again and the primordium resumed its migration (Figure 5A, Figure 5 – Video 1). Thus, a pulse of zGrad expression can deplete Cxcr4b-EGFP to levels unable to sustain directed cell migration of the primordium. This suggests that temporal zGrad induction from the heat shock promoter can be used to induce reversible protein loss of function scenarios.

Fourth, we asked whether tissue-specific expression of zGrad from the *cxcr4b* promoter can degrade Cxcr4b-EGFP and recapitulate the *cxcr4b* mutant primordium migration phenotype (25). To address this question, we expressed zGrad from a 69 kb genomic fragment spanning the *cxcr4b* locus (*cxcr4b:zGrad*) (Figure 6A). The expression pattern of *zGrad* mRNA in *cxcr4b:zGrad* embryos faithfully recapitulated the *cxcr4b* mRNA expression pattern (Figure 6B). We crossed this line into the *cxcr4b:cxcr4b-EGFP-IRES-Kate2-CaaX-p1; cxcr4b-/-* background and determined the degree of Cxcr4b-EGFP degradation compared to Kate2-CaaX expression in primordia of *cxcr4b:zGrad* embryos and control embryos. Similar to the *cxcr4b:cxcr4b-EGFP-IRES-Kate2-CaaX-p7* transgenic line used above, the *cxcr4b:cxcr4b-EGFP-IRES-Kate2-CaaX-p1* fully restores primordium migration in *cxcr4b* mutant embryos, however, it expresses Cxcr4b-EGFP at two-fold lower levels (29). This analysis showed that zGrad efficiently depleted Cxcr4b-EGFP below detectable levels (Figure 6C, D). Next, we assessed the primordium migration by

staining for *cxcr4b* mRNA at 38 hpf. In *cxcr4b* mutant control embryos that carried the rescuing *cxcr4b:cxcr4b-EGFP-IRES-Kate2-CaaX-p1* transgene but lacked the *cxcr4b:zGrad* transgene, the primordium completed its migration and deposited the same number of neuromasts with the same spacing as in wild-type embryos (Figure 6E, F, figure supplement 1B). In contrast, embryos with the *cxcr4b:zGrad* transgene migrated on average only 72.5% of the distance (Figure 6E, F). Compared to primordia in *cxcr4b*-/- embryos, which showed little to no directed migration (Figure 6E, F) (25) primordia in *cxcr4b*-/-; *cxcr4b:cxcr4b-EGFP-IRES-Kate2-CaaX-p1*; *cxcr4b:zGrad* embryos migrated directionally but at reduced speed, did not fully complete their migration and failed to deposit the terminal neuromasts by 4 dpf (Figure 6E, F – figure supplement 1B, C). Importantly, expression of zGrad in the primordium did not affect its migration (Figure 6 – figure supplement 1A). This suggests that zGrad expression from the *cxcr4b* promoter efficiently degrades Cxcr4b-EGFP to levels low enough to slow primordium migration but not low enough to recapitulate the primordium migration defect observed in embryos with loss of Cxcr4b function, probably because the *cxcr4b* promoter does not express zGrad at high enough levels for complete degradation of Cxcr4b-EGFP driven from the same promoter. More generally, these observations indicate that expression of zGrad from a tissue-specific promoter can result in efficient degradation of GFP-tagged proteins to levels low enough to perturb protein function and cause tissue-specific defects.

## Discussion

In our study, we sought to develop a tool that allows for the acute inactivation of proteins in zebrafish. We modified the anti-GFP nanobody-based deGradFP system from flies (9) and adapted it to zebrafish and named it zGrad. zGrad efficiently degrades GFP-tagged transmembrane, cytoplasmic and nuclear proteins. It recognizes different GFP versions (EGFP, sfGFP and Citrine, Figure 1 and 2) and targets the tagged proteins for degradation. In contrast

to other degron systems (2) and similar to deGradFP (7), zGrad degraded proteins tagged at the N-terminus, embedded within the protein and at the C-terminus in the examples reported here (Figure 1 and 2). We found that zGrad rapidly degrades GFP-tagged proteins with half-lives of around 20 min for transmembrane and cytoplasmic proteins (Figure 2 and Table 2). These kinetics are similar to the kinetics reported for other degron-based systems (5, 11, 13). The degradation of H2A-EGFP was significantly slower displaying a half-life of about 2.5 h (Figure 2 and Table 2). This is could be due to the long life-time of histone proteins (30) and the possibility that protein degradation is less efficient in nuclei. Importantly, in our system zGrad expression needs to be induced. This delays the onset of degradation by 65 to 200 min for the proteins we investigated. Nevertheless, zGrad degrades proteins rapidly enough to assess the consequences of abrupt protein inactivation.

One simple use of zGrad is the study of the contribution of maternally supplied proteins in early development. Depletion of maternal proteins by expressing zGrad from injected mRNA should uncover early protein requirements and can circumvent the laborious process of generating maternal mutants for essential genes by germline replacement (31). Our finding that the depletion of maternal Ctnna results in an early and severe cell-cell adhesion defect is consistent with this idea (Figure 3). Alternatively, a pulse of zGrad should allow one to dissect the temporal requirements of proteins. Depending on the protein function this could result in a reversible phenotype as observed when we transiently stalled the migration of the primordium by depleting Cxcr4b (Figure 5) or to an irreversible phenotype if the function of the protein is continually required for viability as observed when we depleted Cdh1 and disrupted the integrity of the embryo (Figure 4). Another use of zGrad is to deplete proteins from certain tissues. By expressing zGrad from tissue-specific promoters, one can circumvent essential early requirements, assess later protein functions and disentangle the contribution of tissues to

complex phenotypes. Our observation that depletion of Cxcr4b in the primordium by expressing zGrad from the *cxcr4b* promoter results in slowed migration supports this idea (Figure 6).

An important consideration is that zGrad needs to be expressed at high enough levels to deplete proteins to sufficiently low levels to fully disrupt protein function. One way to achieve high tissue-specific zGrad expression is to amplify the production of zGrad through such systems as Gal4/UAS (32) or – to also add temporal control – inducible systems such as the Tet-On system (33). Such modifications combined with the increasing number of GFP-tagged transgenic (15, 34) and knock-in lines (35) should render zGrad as a useful tool for the study of the consequences of acute loss of protein function in zebrafish, possibly also circumventing the problem of genetic compensation observed in studies of genetic mutants (36).

## Materials and Methods

### Zebrafish strains

Embryos were staged as previously described (37). Hours post fertilization (hpf) was used to determine the developmental age of the embryos. Embryos were incubated at 28.5 °C from one-cell-stage (0 hpf) until the indicated time. *cxcr4b*$^{t26035}$ (38) homozygous mutant embryos were generated by inbreeding heterozygous adults, crossing homozygous adult with heterozygous adults or inbreeding homozygous adults. *tg(cxcr4b:cxcr4b-EGFP-IRES-Kate2-CaaX)* (27, 28) embryos were generated by crossing heterozygous adults with wild-type adults and sorted by GFP expression. *Gt(ctnna-citrine)Ct3a* (15) lines were maintained by inbreeding of heterozygous adults or homozygous adults. *cdh1*(*tx230*) (22) were kept as heterozygous adults and *cdh1* homozygous embryos were generated by inbreeding heterozygous adults. The *hsp70:sec-mCherry* (39), *cxcr4b:cxcr4b-EGFP-IRES-Kate2-CaaX-p1* (28), *cxcr4b:cxcr4b-EGFP-IRES-Kate2-CaaX-p7* (27), *cxcr4b:H2A-EGFP* (40) and *cxcr4b:H2A-mCherry* (39) were

370 previously described. Zebrafish were maintained under the approval from IACUC (protocol
371 number: 170105-02).
372
373 **Generation of transgenic animals**
374 *hsp70l:zGrad-IRES-h2a-TagBFP*
375 *zGrad*, *IRES-h2a* and *TagBFP* sequences were amplified by PCR and cloned into the plasmid
376 *pDEST-tol2-hsp70l* (41) by Gibson assembly (42). *pDEST-tol2-hsp70l* contains a genomic
377 fragment spanning 1.5 kb upstream of the *hsp70l* start codon (43). 50 ng/µl of the *pDEST-tol2-*
378 *hsp70l-zGrad-IRES-TagBFP* plasmid was co-injected with 25 ng/µl *tol2* mRNA into one-cell-
379 stage embryos. Founder fish were identified by *in situ* hybridization against *vhhgfp4* sequence
380 of heat-shocked offspring. Briefly, adult fish that were injected as embryos were outcrossed with
381 wild-type adults and embryos were collected. At the shield stage, the embryos were heat-
382 shocked at 39.5 °C for 30 min. Preparation of the antisense RNA probe and whole-mount *in situ*
383 hybridization were performed as previously described (38). Fish that gave rise to *hsp70l:zGrad-*
384 *IRES-H2A-TagBFP* offspring were kept as founder fish. zGrad activity was confirmed by heat
385 shocking *hsp70l:zGrad-IRES-H2A-TagBFP; cxcr4b:h2a-EGFP* embryos and observation of
386 H2A-GFP degradation. The line from the founder that showed the strongest GFP degradation
387 was kept and used in this study. The full name of this line is *tg(hsp70l:zGrad-IRES-H2A-*
388 *TagBFP)p1.* Note H2A-TagBFP expression from the IRES is not detectable in this line.
389
390 *cxcr4b:zGrad-IRES-h2a-TagBFP*
391 For the *cxcr4b:zGrad-IRES-h2a-TagBFP* BAC transgene, we used the BAC clone DKEY-
392 169F10 (44). This BAC clone contains the *cxcr4b* locus. We modified this BAC in two ways by
393 recombineering. First, we modified pBS-IndHom-Tol2-FRT-GalK-cryaa-dsRed (Addgene
394 plasmid # 73203, (29)) by replacing the cryaa:dsRed sequence with *myl7:mScarlet* and the
395 FRT-GalK-FRT sequence with the kanR sequence. The *myl7* (synonym *cmlc2*) promoter drives

396 expression in the myocardium (45) and kanR allows for rapid kanamycin-based selection of
397 recombinants. The full name of this plasmid is *pBS-IndHom-Tol2(exon4)-Kan-Tol2(exon1)-*
398 *myl7:mScarlet-Hom*. We amplified *Tol2(exon4)-Kan-Tol2(exon1)- myl7:mScarlet* cassette by
399 PCR and inserted it into the pIndigoBAC-5 backbone of the DKEY-169F10 BAC clone using
400 *kanamycin* as a selection marker. Second, a cassette containing *zGrad-IRES-h2a-TagBFP-*
401 *FRT-galK-FRT* flanked by homology arms upstream of the *cxcr4b* exon2 and downstream of the
402 *cxcr4b* stop codon was inserted to replace the *cxcr4b* coding sequence in exon2 using *galK* as
403 a selection marker. The *galK* cassette was removed by Flippase. The obtained BAC was
404 characterized with sequencing the modified region in the BAC and EcoRI finger printing. This
405 transgene expresses zGrad-IRES-H2A-TagBFP fused to 5 amino acids from *cxcr4b* exon1
406 under the *cxcr4b* promoter. The BAC was prepared with the nucleobond BAC 100 kit
407 (Clonetech) and co-injected with 25 ng/µl *tol2* mRNA into one-cell-stage embryos. Stable
408 transgenic animals were identified by out-crossing injected adults and screening for the red
409 hearts in 4 dpf larvae. Embryos were collected from each stable transgenic fish and tested for
410 expression of *zGrad* by whole mount *in situ* hybridization 30 hpf. We selected the transgenic line
411 that expressed the highest level of *zGrad* from the BAC transgene and used it in this study. The
412 full name of this transgenic line is *TgBAC(cxcr4b:zGrad-IRES-h2a-TagBFP)p3*. Note H2A-
413 TagBFP expression from the IRES is not detectable in this line.
414
415 For the *hsp70l:sec-GFP* transgene, the *pDestTol2pA-hsp70l-anos1b-sv40pA* plasmid was used
416 as a template (39). Using Gibson cloning (42), we replaced the *anos1b* coding sequence with
417 the coding sequence of *GFP* fused to the 3' end of the *fgf3* secretion signal (amino acids 1 to
418 18). We verified the final construct by sequencing and co-injected it along with *tol2* transposase
419 mRNA into zebrafish embryos at the one-cell stage. Stable transgenic fish were identified by
420 out-crossing adults injected with the transgene and raising larvae from fish whose offspring
421 were identified to express GFP upon heat shock as determined by green fluorescence. Founder

422 fish were verified to carry a single copy of the transgene by determining the fraction of progeny
423 carrying the transgene. The full name of this transgenic line is *Tg(hsp70l:sec-GFP)p1*.
424
425 *cdh1:cdh1-sfGFP* and *cdh1:cdh1-TagRFP* lines
426 For the *cdh1:cdh1-sfGFP* and *cdh1:cdh1-TagRFP* BAC transgenes, we used the BAC clone
427 CHORI-211-175C23. This BAC clone spans 72 kb of genomic sequence and contains the *cdh1*
428 locus and was modified in two ways by recombineering. First, the *Tol2* sites and the
429 *cryaa:Cerulean* transgenesis marker were inserted into the BAC backbone (29). Second, a
430 cassette consisting of *sfGFP-FRT-galK-FRT* or *TagRFP-FRT-galK-FRT* flanked by 446 bp and
431 590 bp of homology upstream of the stop codon in *cdh1* exon 16, and downstream of the stop
432 codon in *cdh1* exon 16, respectively, was inserted before the *cdh1* stop codon using galK-
433 mediated recombineering (46). The galK cassette was removed by Flippase-mediated
434 recombination. This transgene expresses the full length of Cdh1 fused to sfGFP or TagRFP
435 from the *cdh1* promoter. The final BAC transgenes were characterized by EcoRI restriction
436 digestion and sequencing of PCR amplicons of the modified locus. The CHORI-211-175C23
437 BAC clone was obtained from BACPAC Resources, Children' Hospital Oakland Research
438 Institute, CA, USA (bacpacorders@chori.org). The BACs were purified with the nucleobond
439 BAC 100 kit (Clontech). We co-injected 1 nl of 40 ng/µl *Tol2* mRNA and 50–250 ng/µl of the
440 *cdh1:cdh1-sfGFP* or *cdh1:cdh1-TagRFP* BAC transgene DNA into the lifting cell of the zygote of
441 0 to 20-minute old embryos. The *Tol2* mRNA was transcribed from the pCS2FA-transposase
442 plasmid (41) using the mMessage mMachine SP6 Transcription Kit (Thermo Fisher). Stable
443 transgenic larvae were identified by out-crossing adults injected with the *cdh1:cdh1-sfGFP* or
444 *cdh1:cdh1-TagRFP* BAC transgenes, and by raising larvae positive for the blue fluorescent
445 transgenesis marker in the lens of the eye at 4 dpf. The full names of these two transgenic lines
446 are *TgBAC(cdh1:cdh1-sfGFP)p1* and *TgBAC(cdh1:cdh1-TagRFP)p1*.
447

448 **Generation of plasmids for *in vitro* transcription**

449 To construct *pCS2+-mScarlet-V5*, the *mScarlet* coding sequence was amplified from pmScarlet-
450 C1 (Addgene plasmid # 85042, (47)) by PCR with a 5' primer containing V5-tag sequence and
451 cloned into *pCS2+* plasmid by Gibson assembly. To construct *pCS2+-sfGFP*, *sfGFP* coding
452 sequence was amplified by PCR and cloned into *pCS2+* plasmid by Gibson assembly.
453 To construct *pCS2+-Nslmb-vhhGFP4*, *Nslmb-vhhGFP4* coding sequence was amplified from
454 *pcDNA3-NSlmb-vhhGFP4* (Addgene plasmid #35579, (7)) by PCR and cloned into *pCS2+*
455 plasmid by Gibson assembly.
456 To construct *pCS2+-OsTIR1-mCherry*, the *OsTIR1* and *mCherry* coding sequences were
457 amplified from *pMK232-CMV-OsTIR1-PURO* (Addgene plasmid #72834, (10)) and *pCS2+-*
458 *lyn$_2$mCherry* (kind gift from Reinhard Köster and Scott Fraser) respectively, by PCR and cloned
459 into *pCS2+* plasmid by Gibson assembly.
460 To construct *pCS2+-sfGFP-mAID*, the *sfGFP* coding sequence was amplified by PCR and the
461 mAID tag sequence (48) was generated by primer annealing and cloned into *pCS2+* plasmid by
462 Gibson assembly.
463 To construct *pCS2+-fbxw11b-vhhGFP* (*pCS2+-zGrad*), the coding sequence for the N-terminal
464 217 amino acids of Fbxw11b was amplified by PCR from cDNA of 36 hpf embryos, fused to the
465 *vhhGFP4* coding sequence and inserted into the *pCS2+* plasmid by Gibson assembly.
466 To construct *pCS2+-zif1*, the coding sequence of *zif1* was codon optimized for zebrafish by
467 gene synthesis (IDT) and inserted into the *pCS2+* plasmid by Gibson assembly.
468 To construct *pCS2+-sfGFP-ZF1*, the coding sequence of *ZF1* was codon optimized for zebrafish
469 by gene synthesis (IDT) and inserted together with *sfGFP* into the *pCS2+* plasmid by Gibson
470 assembly.
471 The *pCS2+-vhhGFP4-hSPOP* and *pCS2+-vhhGFPmut-hSPOP* plasmids were previously
472 described (4).
473

474 **mRNA injection**

475 Templates for *in vitro* mRNA transcription were generated by PCR or restriction digest of mRNA
476 expression plasmids. mRNAs were transcribed using the mMESSAGE mMACHINE SP6
477 transcription Kit (Thermo Fisher Scientific). Injection mixes contained 50 ng/µl mRNAs except
478 for the mAID experiment, where *OsTIR1-mCherry* mRNA was prepared as 10 ng/µl, 5 ng/µl and
479 1 ng/µl, with 0.1% Phenol Red Solution (LIFE TECHNOLOGIES). The injection mix was injected
480 in one-cell-stage embryos. mRNA quality was assessed after injection through gel
481 electrophoresis by collecting the remaining mix in the injection needle assessing intactness of
482 mRNA.

483

484 **Auxin inducible degradation**

485 Natural auxin 3-Indoleacetic acid (IAA, Sigma Aldrich) was dissolved in 100% ethanol at a
486 concentration of 250 mM, protected from light and stored at -20 °C. Injected embryos were
487 raised in fish water (4g/l instant ocean salt) without Methylene blue to avoid possible
488 interference from the dye. 50 ng/µl *sfGFP-mAID* mRNA was co-injected with 10 ng/µl, 5 ng/µl or
489 1 ng/µl *OsTIR1-mCherry* mRNA. Injected embryos were dechorionated manually. At 8 hpf IAA
490 was added to 500 µM final concentration (5, 49). Images were taken on a Leica 165M FC
491 Fluorescent Stereo Microscope equipped with a Leica DFC345 FX camera every hour for 3
492 hours.

493

494 **Image acquisition and quantification of mRNA-injected embryos**

495 To quantify the ratio of sfGFP-ZF1 fluorescence to mScarlet-V5 fluorescence, injected embryos
496 were dechorionated manually or by adding Pronase (Sigma Aldrich) to 0.3 mg/ml on petri dishes
497 coated with 2% agarose in fish water at 10 hpf. Injected embryos were mounted in 0.5% low-
498 melt agarose (National Diagnostics)/Ringer's solution (MgSO4 0.6 mM, CaCl2 1 mM, KCl 5 mM,
499 NaCl 111 mM, HEPES 5 mM) on a slide. Mounted embryos were imaged on Leica SP5 II

confocal microscope equipped with HyD detectors (Leica Microsystems) using a Leica 20x (NA 0.7) objective and a Leica 40x water immersion lens (NA 1.1) in the case of vhhGFP4-hSPOP-mediated GFP degradation.

All images were collected in the photon-counting mode with identical microscope settings. Quantification of signal intensity from injected embryos was performed using a custom-written ImageJ macro (Data File 1). Briefly, the macro selects a single Z-slice and generates a mask based on the mScarlet intensities using the Otsu thresholding algorithm. The mScarlet mask is then applied to the green and red channels of the same Z-slice to extract average GFP and mScarlet signal intensities only from the masked region. These procedures is repeated on the whole Z-stack. Average signal intensities from the first 40 Z-slices (62 µm) starting at the animal pole were used to calculate the green-to-red fluorescence intensity ratio of an embryo. The sfGFP-ZF1/mScarlet-V5 fluorescence intensity ratios for vhhGFP4-hSPOP-mediated GFP degradation were calculated manually using ImageJ. Briefly, five nuclei per embryo were outlined and the average nuclear signal intensities in the green and red channels was extracted and used for the calculation of the green-to-red fluorescence intensity ratios in the nuclei. For quantification of signal intensities in the cytoplasm, a 20 x 20 pixels (3.79 µm x 3.79 µm) region was manually selected and the average signal intensities in the green and red channels were extracted to calculate the green-to-red fluorescence intensity ratio. The regions from five cells per embryo for five embryos were analyzed for each condition. The overview fluorescence images in Figure 1 – figure supplements 1A (AID) were collected on Leica 165M FC Fluorescent Stereo Microscope equipped with a Leica DFC345 FX camera.

**Heat shock regimens**

To determine the degradation kinetics of H2A-EGFP, *cxcr4b:h2a-EGFP; cxcr4b:h2a-mCherry* embryos with and without the *hsp70l:zGrad-IRES-h2a-TagBFP* transgene were heat shocked

around 29-30 hpf at 39.5 °C for one hour in a water bath and imaged 80 min after the end of heat shock every 10 min for 9.5 hours on a Leica SP5 II confocal microscope equipped with HyD detectors (Leica Microsystems) using a 20x (NA 0.5) objective. Laser power was calibrated as 30 µW for 488 and 120 µW for 561. Pinhole was set to 85 µm.

To determine the degradation kinetics of Cdh1-sfGFP, *cdh1:cdh1-sfGFP; cdh1:cdh1-TagRFP* embryos with and without the *hsp70l:zGrad-IRES-h2a-TagBFP* transgene were mounted in the 0.5% low-melt agarose/Ringer's solution with tricane, heat shocked around 31 hpf at 39.5 °C for 30 min in a water bath and imaged 35 min after the end of heat shock every 10 min for 4.8 hours on a Leica SP5 II confocal microscope equipped with HyD detectors (Leica Microsystems) using a 40x (NA 0.8) objective. The laser power was calibrated to 32 µW for the 488 nm laser line and 115 µW for the 594 nm laser line. The pinhole was set to 230 µm.

To determine the degradation kinetics of Ctnna-Citrine, *ctnna:ctnna-Citrine/+* embryos with or without the *hsp70l:zGrad-IRES-h2a-TagBFP* transgene were mounted in the 0.5% low-melt agarose/Ringer's solution with tricane, heat shocked around 31 hpf at 39.5 °C for 30 min in a water bath and imaged 35 min after the end of the heat shock every 20 min for 8 hours on a Leica SP8 confocal microscope equipped with HyD detectors (Leica Microsystems) using a 40x (NA 0.8) objective. The laser power was set to 31 µW for the 488 nm laser line. The pinhole was set to 106 µm. Imaged embryos were genotyped for *hsp70l:zGrad-IRES-h2a-TagBFP* by PCR.

To test the degradation of Sec-GFP by zGrad, *hsp70l:sec-GFP; hsp70:sec-mCherry* with and without the *hsp70l:zGrad-IRES-h2a-TagBFP* transgene were heat shocked around 24 hpf at 39.5 °C for one hour in a water bath. Embryos were imaged at 30 hpf with a Leica 165M FC Fluorescent Stereo Microscope equipped with a Leica DFC345 FX camera. Imaged embryos were digested and genotyped for *hsp70l:zGrad-IRES-h2a-TagBFP* by PCR.

To observe the consequences of transient loss of Cxcr4b function, *cxcr4b:cxcr4b-EGFP-IRES-Kate2-CaaX-p7; cxcr4b -/-* embryos with and without the *hsp70l:zGrad-IRES-h2a-TagBFP* transgene were heat shocked at 31 hpf and 39.5 °C for one hour in a water bath and imaged 30 min after the end of the heat shock every 20 min for 8 hours on a Leica SP8 confocal microscope equipped with HyD detectors (Leica Microsystems) using a 20x (NA 0.5) objective. The laser power was adjusted to 31 µW for the 488 nm laser line and to 73 µW for 594 nm laser line. The pinhole was set to 85 µm. Imaged embryos were genotyped for *hsp70l:zGrad-IRES-h2a-TagBFP* by PCR as described below.

**Analysis of the degradation kinetics after heat shock**

Quantification of signal intensity from heat shocked embryos was performed using a custom-written ImageJ macro (Data File 2). For H2A-EGFP/H2A-mCherry ratio imaging, a region encompassing the primordium and the somites (100 x 50 pixels, 75.76 µm x 37.88 µm) was manually selected. The macro script duplicates the red channel, applies a Gaussian Blur (sigma = 1) and generates a mask based on the mCherry intensities using Renyi Entropy Thresholding algorithm for the primordium and the imageJ Default Thresholding for the somites. Then, the macro applies the mask on the green and red channels to extract H2A-EGFP and H2A-mCherry signal intensities only from the masked region. Then, the macro sum-projects the green and red channels and extracts mean intensities of H2A-EGFP and H2A-mCherry for each time point. Data from two independent imaging sessions were pooled for the analysis. Four embryos with *hsp70l:zGrad* transgene (two from each imaging session) and four embryos without *hsp70l:zGrad* transgene as control (two from each imaging session) were analyzed.

For Cdh1-sfGFP/Cdh1-TagRFP ratio imaging, first a region of 300 x 300 pixel (77.27µm x 77.27 µm) at the center of the embryo was manually selected. The macro duplicates the red channel, applies a Gaussian Blur (sigma = 1) and generates a mask based on the TagRFP intensities using the imageJ Default Thresholding. Then, it applies the mask on the green and red

channels to extract Cdh1-sfGFP and Cdh1-mCherry signal intensities only from the masked region. Then, the macro sum-projects the green and red channels and extracts the mean intensities of the Cdh1-sfGFP and Cdh1-TagRFP fluorescences for each time point. Three embryos with carrying the *hsp70l:zGrad* transgene and four control embryos without the *hsp70l:zGrad* transgene were analyzed.

For Ctnna-Citrine fluorescence intensity approximation, a region of 300 x 300 pixel (85.23 x 85.23 µm) at the center of the embryo was manually selected. The Z-stack comprising this region was maximum projected. The mean intensities of maximum-projected images were extracted over all time points. Four embryos with *hsp70l:zGrad* transgene and four embryos without *hsp70l:zGrad* transgene as control were analyzed.

For Cxcr4b-EGFP-to-Kate2-CaaX ratio imaging, the region of the primordium was manually selected and signal intensities were quantified using a custom-written ImageJ macro (Data File 3). Briefly, the macro script duplicates the red channel, applies a Gaussian Blur (sigma = 2), maximum-projects the Z-stack, generates a mask based on the Kate2 intensities using the imageJ Default Thresholding, fills holes, erodes and dilates once (erosion and dilation reduces noise). Then, the macro sum-projects the green and red channels and applies the mask to the green and red channels to extract Cxcr4b-EGFP and Kate2-CaaX signal intensities only from the masked regions for each time point. Five embryos with *hsp70l:zGrad* transgene and five embryos without *hsp70l:zGrad* transgene as control were analyzed.

**Analysis of the circularity of the primordium**

To quantify the morphology of the primordium, we defined the extension of the primordium as the first 100 µm from the tip of the primordium. Using Fiji, the primordium region was manually cropped in the red channel based on the Kate2-CaaX fluorescence intensities. Then, a median filter (6 pixels) was applied and the background was subtracted. Images were rendered binary using the Huang thresholding algorithm to obtain clear outlines of the primordium. Finally, we

603 quantified the circularity of the primordium for each time point using the “Analyze Particles”
604 macro in Fiji. The circularity is defined as *circularity = 4pi(area/perimeter^2)*.
605
606 **Cumulative migration distance and kymographs analysis**
607 To quantify the migration distance of the primordium over time, the “Manual Tracking” plugin in
608 Fiji was used to track the tip of the primordium. Kymographs were drawn using the
609 “KymoResliceWide” plugin in Fiji with a width of 5 pixel.
610
611 **Image acquisition and quantification of zGrad-mediated Cxcr4b-EGFP degradation with**
612 **zGrad expressed from the *cxcr4b* promoter**
613 *cxcr4b:cxcr4b-EGFP-IRES-Kate2-CaaX-p1* embryos and *cxcr4b:cxcr4b-EGFP-IRES-Kate2-*
614 *CaaX-p1*; *cxcrb4:zGrad-IRES-h2a-TagBFP* embryos were sorted for the expression of the
615 transgenesis marker (the *cxcr4b:cxcr4b-EGFP-IRES-Kate2-CaaX-p1* transgene expresses
616 dsRed in the lens and the *cxcrb4:zGrad-IRES-h2a-TagBFP* transgene expresses mScarlet in
617 the myocardium of the heart) at 29 hpf. Ten embryos of each genotype were mounted in 0.5 %
618 low-melt agarose/Ringer’s solution with tricane on a slide. Embryos were imaged at 33 to 34 hpf
619 using a Leica SP8 confocal microscope equipped with HyD detectors (Leica Microsystems)
620 using a 40x (NA 1.1) objective. The laser power was calibrated to 27 μW for the 488 nm laser
621 line and 82 μW for the 594 nm laser line. The pinhole was set to 77.17 μm. To quantify the
622 signal intensity ratio of EGFP/Kate2 in the primordium, the primordium was manually selected
623 and fluorescent intensities for EGFP and Kate2 were extracted using the same custom-written
624 ImageJ macro as described in the quantification of Cdh1-sfGFP degradation kinetics.
625
626 **Degradation of Ctnna-Citrine by zGrad mRNA injection**
627 1-2 nl of 50 ng/μl of *zGrad* mRNA or 50 ng/μl of *sfGFP* mRNA were injected in one-cell stage
628 zygotic *ctnna:ctnna-Citrine*; *ctnna:ctnna-Citrine* and maternal zygotic *ctnna:ctnna-Citrine*;

629 *ctnna:ctnna-Citrine* embryos. Possible degradation of the mRNA in the injection mix was
630 assessed by electrophoresis of the injection mix in the needle after injection of the embryos. For
631 imaging, the embryos were mounted in 0.5% low-melt agarose/Ringer's solution on a slide.
632 Images of injected embryos were obtained using an Axioplan Microscope (Zeiss) equipped with
633 an Axiocam (Zeiss) and a 10x (NA 0.5) objective for Figure 3B and 4E and a 5x (NA 0.25)
634 objective for Figure 3H. The number of dead and alive embryos was scored at 24 hpf.
635
636 **Genotyping of *cxcr4b*$^{t26035}$ and *hsp70l:zGrad-IRES-H2A-TagBFP***
637 To distinguish endogenous *cxcr4b -/+* and *cxcr4b -/-* from the *cxcr4b:cxcr4b-EGFP-IRES-kate2-*
638 *CaaX* transgene in Figure 6 and Figure 6 – figure supplement 1, the following outer and nested
639 primer pairs were used:
640 forward outer primer: GCAGACCTCCTGTTTGTCC
641 reverse outer primer: CTAAGTGCACACATACACACATT
642 forward nested primer: TCGAGCATGGGTACCATC
643 reverse nested primer: CTTAATCATCCATGTGGAAAAG
644 The reverse primers are designed to anneal to 3'UTR of the *cxcr4b* gene so that *cxcr4b-EGFP-*
645 *IRES-Kate2-CaaX* transgene will not be amplified due to its large size. The PCR product was
646 digested with the restriction enzyme HpyAV (NEB) to distinguish heterozygous and
647 homozygous mutants.
648 To genotype *hsp70l:zGrad-IRES-H2A-TagBFP*, the region between *hsp70l* promoter and
649 *fbxw11b* was amplified by PCR using the following outer and nested primer pairs:
650 forward outer primer: TGAGCATAATAACCATAAATACTA
651 reverse outer primer: ACCAGTTGGACTTGATCCATATGTCGACCACACCTCCAG
652 forward nested primer: AGCAAATGTCCTAAATGAAT
653 reverse nested primer: CAGAGGTGTTCATCTGCTC.
654

**Whole-mount *in situ* hybridization**

The procedures for RNA probe synthesis and whole-mount *in situ* hybridization were done as previously described (50). The RNA probe against *cxcr4b* was previously described (38). The template for the synthesis of the in situ RNA probe against vhhGFP4 was amplified from *pcDNA3-NSlmb-vhhGFP4* (Addgene plasmid #35579) using the following primer pair:

forward primer: ggccgtcgacATGATGAAAATGGAGACTGAC

reverse primer: TAATACGACTCACTATAGGGTTAGCTGGAGACGGTGACCTG

The RNA probe was synthesized using the Roche DIG labeling mix (Roche) and detected with an anti-DIG antibody coupled to alkaline phosphatase (1:5000, Roche) and NBT/BCIP stain (Roche). Embryos were mounted in the 3% Methyl cellulose (Sigma Aldrich). Images were collected on a Axioplan Microscope (Zeiss) equipped with an Axiocam (Zeiss) using a 10x (NA 0.5) objective.

**Quantification of the primordium migration distance**

*cxcr4b:cxcr4b-EGFP-IRES-Kate2-CaaX-p1; cxcr4b -/+* fish were crossed to *cxcrb4:zGrad-IRES-h2a-TagBFP; cxcr4b -/-* fish and embryos were sorted based on the transgenesis markers (dsRed in lens for *cxcr4b:cxcr4b-EGFP-IRES-Kate2-CaaX-p1* and mScarlet in myocardim of heart for *cxcrb4:zGrad-IRES-h2a-TagBFP*) at 38 hpf and fixed in 4% PFA (Sigma Aldrich) in PBST overnight at room temperature. Whole-mount *in situ* hybridization against *cxcr4b* mRNA was performed as described above. Images for quantification of migration distance were taken in PBST on an Axioplan Microscope (Zeiss) equipped with an Axiocam (Zeiss) using a 10x (NA 0.5) objective. Both sides of the embryo were imaged and counted as individual replicates. Images for Figure 6E were taken by mounting embryos in 3% Methyl cellulose. *cxcr4b* mutant embryos were genotyped by PCR after image acquisition. The migrating distance of the primordium was quantified manually using ImageJ.

**Conditional Cdh1 loss-of-protein function through zGrad expression from a heat shock promoter**

The number of embryos from *cdh1:cdh1-sfGFP; cdh1 +/-* with or without *hsp70l:zGrad* females crossed with *cdh1 +/-* males was counted at 5 hpf. The dead embryos were removed at 24 hpf and embryos were sorted by Cdh1-sfGFP expression. At 25 hpf, embryos were heat shocked at 39.5 °C for one hour in a water bath. The embryos were mounted in 0.5% low-melt agarose/Ringer's solution on a slide. Images of embryos were recorded with an Axioplan Microscope (Zeiss) equipped with an Axiocam (Zeiss) and a 5x (NA 0.25) objective (panels B and C in Figure 4) and a 10x (NA 0.5) objective (panels D and E in Figure 4). The number of embryos with and without skin defects and lethality was scored at 32 hpf.

**DASPEI staining and neuromast position quantification**

The location of neuromasts was assessed by staining 4 dpf live embryos with 25 ug/mL DASPEI (2-(4-(dimethylamino)styryl)-N-Ethylpyridinium Iodide, Invitrogen). Images were collected on Leica 165M FC Fluorescent Stereo Microscope equipped with a Leica DFC345 FX camera. The location of the last neuromast on the trunk was quantified as ratio between the length from the head to the last neuromast on the trunk divided by the length of the whole embryo (see Figure 6 – figure supplement 1B, C).

**Statistical analysis**

Statistical tests were performed using R and R-studio software. To compare two sample sets, first each sample set was tested using the Kolmogorov-Smirnov test to determine whether the sample set was normally distributed. Then, we tested whether the sample sets had the same standard deviation using the F-test. Based on the result of F-test, the two sample sets were compared by either the Welch's t-test or the Student's t-test (Figure 1D, Figure 1 – figure supplements 2B, 3C, 6D, 6F, Figure 6 – figure supplement 6C). To analyze the fold-change

curves in Figure 2C, 2E, 2H, 2K, the curves were fitted to a one-exponential decay model (Y = Span*exp(-k*X)+Plateau) using Prism 7 (Graphpad). The values of T1/2 and the plateau, which we assumed to be the value of maximal degradation, were extracted from the fitted curves. In Figure 5D (inset, 30 min to 240 min), two data sets were compared by paired-t test using Prism.

**Acknowledgements**

We thank S. Lau for critical comments; D. Kane, L. Trinh and S. Fraser for reagents, T. Gerson for excellent fish care and Dorus Gadella (Addgene plasmid # 85042), Markus Affolter (Addgene plasmid # 35579) and Masato Kanemaki (Addgene plasmid # 72835) for plasmids. This work was supported by NIH grants HD088779 (H.K.) and NS102322 (H.K.).

**Competing interests**

The authors declare no competing interest.

## References

1. Housden BE, Muhar M, Gemberling M, Gersbach CA, Stainier DY, Seydoux G, et al. Loss-of-function genetic tools for animal models: cross-species and cross-platform differences. Nat Rev Genet. 2017;18(1):24-40.

2. Natsume T, Kanemaki MT. Conditional Degrons for Controlling Protein Expression at the Protein Level. Annu Rev Genet. 2017;51:83-102.

3. Bonger KM, Rakhit R, Payumo AY, Chen JK, Wandless TJ. General method for regulating protein stability with light. ACS Chem Biol. 2014;9(1):111-5.

4. Shin YJ, Park SK, Jung YJ, Kim YN, Kim KS, Park OK, et al. Nanobody-targeted E3-ubiquitin ligase complex degrades nuclear proteins. Sci Rep. 2015;5:14269.

5. Daniel K, Icha J, Horenburg C, Muller D, Norden C, Mansfeld J. Conditional control of fluorescent protein degradation by an auxin-dependent nanobody. Nat Commun. 2018;9(1):3297.

6. Neklesa TK, Tae HS, Schneekloth AR, Stulberg MJ, Corson TW, Sundberg TB, et al. Small-molecule hydrophobic tagging-induced degradation of HaloTag fusion proteins. Nat Chem Biol. 2011;7(8):538-43.

7. Caussinus E, Kanca O, Affolter M. Fluorescent fusion protein knockout mediated by anti-GFP nanobody. Nat Struct Mol Biol. 2011;19(1):117-21.

8. Wang S, Tang NH, Lara-Gonzalez P, Zhao Z, Cheerambathur DK, Prevo B, et al. A toolkit for GFP-mediated tissue-specific protein degradation in C. elegans. Development. 2017;144(14):2694-701.

9. Brauchle M, Hansen S, Caussinus E, Lenard A, Ochoa-Espinosa A, Scholz O, et al. Protein interference applications in cellular and developmental biology using DARPins that recognize GFP and mCherry. Biol Open. 2014;3(12):1252-61.

748 10. Natsume T, Kiyomitsu T, Saga Y, Kanemaki MT. Rapid Protein Depletion in Human
749 Cells by Auxin-Inducible Degron Tagging with Short Homology Donors. Cell Rep.
750 2016;15(1):210-8.
751 11. Nishimura K, Fukagawa T, Takisawa H, Kakimoto T, Kanemaki M. An auxin-based
752 degron system for the rapid depletion of proteins in nonplant cells. Nat Methods.
753 2009;6(12):917-22.
754 12. Holland AJ, Fachinetti D, Han JS, Cleveland DW. Inducible, reversible system for the
755 rapid and complete degradation of proteins in mammalian cells. Proc Natl Acad Sci U S A.
756 2012;109(49):E3350-7.
757 13. Armenti ST, Lohmer LL, Sherwood DR, Nance J. Repurposing an endogenous
758 degradation system for rapid and targeted depletion of C. elegans proteins. Development.
759 2014;141(23):4640-7.
760 14. Chong SW, Emelyanov A, Gong Z, Korzh V. Expression pattern of two zebrafish genes,
761 cxcr4a and cxcr4b. Mech Dev. 2001;109(2):347-54.
762 15. Trinh le A, Hochgreb T, Graham M, Wu D, Ruf-Zamojski F, Jayasena CS, et al. A
763 versatile gene trap to visualize and interrogate the function of the vertebrate proteome. Genes
764 Dev. 2011;25(21):2306-20.
765 16. Zigman M, Trinh le A, Fraser SE, Moens CB. Zebrafish neural tube morphogenesis
766 requires Scribble-dependent oriented cell divisions. Curr Biol. 2011;21(1):79-86.
767 17. Kofron M, Spagnuolo A, Klymkowsky M, Wylie C, Heasman J. The roles of maternal
768 alpha-catenin and plakoglobin in the early Xenopus embryo. Development. 1997;124(8):1553-
769 60.
770 18. Han MK, Hoijman E, Noel E, Garric L, Bakkers J, de Rooij J. alphaE-catenin-dependent
771 mechanotransduction is essential for proper convergent extension in zebrafish. Biol Open.
772 2016;5(10):1461-72.

773 19. Yoshida-Noro C, Suzuki N, Takeichi M. Molecular nature of the calcium-dependent cell-
774 cell adhesion system in mouse teratocarcinoma and embryonic cells studied with a monoclonal
775 antibody. Dev Biol. 1984;101(1):19-27.
776 20. Stephenson RO, Yamanaka Y, Rossant J. Disorganized epithelial polarity and excess
777 trophectoderm cell fate in preimplantation embryos lacking E-cadherin. Development.
778 2010;137(20):3383-91.
779 21. Larue L, Ohsugi M, Hirchenhain J, Kemler R. E-cadherin null mutant embryos fail to form
780 a trophectoderm epithelium. Proc Natl Acad Sci U S A. 1994;91(17):8263-7.
781 22. Kane DA, Hammerschmidt M, Mullins MC, Maischein HM, Brand M, van Eeden FJ, et al.
782 The zebrafish epiboly mutants. Development. 1996;123:47-55.
783 23. Kane DA, McFarland KN, Warga RM. Mutations in half baked/E-cadherin block cell
784 behaviors that are necessary for teleost epiboly. Development. 2005;132(5):1105-16.
785 24. Montero JA, Carvalho L, Wilsch-Brauninger M, Kilian B, Mustafa C, Heisenberg CP.
786 Shield formation at the onset of zebrafish gastrulation. Development. 2005;132(6):1187-98.
787 25. Haas P, Gilmour D. Chemokine signaling mediates self-organizing tissue migration in
788 the zebrafish lateral line. Dev Cell. 2006;10(5):673-80.
789 26. David NB, Sapede D, Saint-Etienne L, Thisse C, Thisse B, Dambly-Chaudiere C, et al.
790 Molecular basis of cell migration in the fish lateral line: role of the chemokine receptor CXCR4
791 and of its ligand, SDF1. Proc Natl Acad Sci U S A. 2002;99(25):16297-302.
792 27. Venkiteswaran G, Lewellis SW, Wang J, Reynolds E, Nicholson C, Knaut H. Generation
793 and dynamics of an endogenous, self-generated signaling gradient across a migrating tissue.
794 Cell. 2013;155(3):674-87.
795 28. Lewellis SW, Nagelberg D, Subedi A, Staton A, LeBlanc M, Giraldez A, et al. Precise
796 SDF1-mediated cell guidance is achieved through ligand clearance and microRNA-mediated
797 decay. J Cell Biol. 2013;200(3):337-55.

798 29. Fuentes F, Reynolds E, Lewellis SW, Venkiteswaran G, Knaut H. A Plasmid Set for
799 Efficient Bacterial Artificial Chromosome (BAC) Transgenesis in Zebrafish. G3 (Bethesda).
800 2016;6(4):829-34.
801 30. Clift D, McEwan WA, Labzin LI, Konieczny V, Mogessie B, James LC, et al. A Method
802 for the Acute and Rapid Degradation of Endogenous Proteins. Cell. 2017;171(7):1692-706 e18.
803 31. Ciruna B, Weidinger G, Knaut H, Thisse B, Thisse C, Raz E, et al. Production of
804 maternal-zygotic mutant zebrafish by germ-line replacement. Proc Natl Acad Sci U S A.
805 2002;99(23):14919-24.
806 32. Scheer N, Campos-Ortega JA. Use of the Gal4-UAS technique for targeted gene
807 expression in the zebrafish. Mech Dev. 1999;80(2):153-8.
808 33. Campbell LJ, Willoughby JJ, Jensen AM. Two types of Tet-On transgenic lines for
809 doxycycline-inducible gene expression in zebrafish rod photoreceptors and a gateway-based
810 tet-on toolkit. PLoS One. 2012;7(12):e51270.
811 34. Kawakami K, Abe G, Asada T, Asakawa K, Fukuda R, Ito A, et al. zTrap: zebrafish gene
812 trap and enhancer trap database. BMC Dev Biol. 2010;10:105.
813 35. Hoshijima K, Jurynec MJ, Grunwald DJ. Precise Editing of the Zebrafish Genome Made
814 Simple and Efficient. Dev Cell. 2016;36(6):654-67.
815 36. Rossi A, Kontarakis Z, Gerri C, Nolte H, Holper S, Kruger M, et al. Genetic
816 compensation induced by deleterious mutations but not gene knockdowns. Nature.
817 2015;524(7564):230-3.
818 37. Kimmel CB, Ballard WW, Kimmel SR, Ullmann B, Schilling TF. Stages of embryonic
819 development of the zebrafish. Dev Dyn. 1995;203(3):253-310.
820 38. Knaut H, Werz C, Geisler R, Nusslein-Volhard C, Tubingen Screen C. A zebrafish
821 homologue of the chemokine receptor Cxcr4 is a germ-cell guidance receptor. Nature.
822 2003;421(6920):279-82.

823 39. Wang J, Yin Y, Lau S, Sankaran J, Rothenberg E, Wohland T, et al. Anosmin1 Shuttles
824 Fgf to Facilitate Its Diffusion, Increase Its Local Concentration, and Induce Sensory Organs.
825 Dev Cell. 2018;46(6):751-66 e12.
826 40. Kozlovskaja-Gumbriene A, Yi R, Alexander R, Aman A, Jiskra R, Nagelberg D, et al.
827 Proliferation-independent regulation of organ size by Fgf/Notch signaling. Elife. 2017;6.
828 41. Kwan KM, Fujimoto E, Grabher C, Mangum BD, Hardy ME, Campbell DS, et al. The
829 Tol2kit: a multisite gateway-based construction kit for Tol2 transposon transgenesis constructs.
830 Dev Dyn. 2007;236(11):3088-99.
831 42. Gibson DG, Young L, Chuang RY, Venter JC, Hutchison CA, 3rd, Smith HO. Enzymatic
832 assembly of DNA molecules up to several hundred kilobases. Nat Methods. 2009;6(5):343-5.
833 43. Halloran MC, Sato-Maeda M, Warren JT, Su F, Lele Z, Krone PH, et al. Laser-induced
834 gene expression in specific cells of transgenic zebrafish. Development. 2000;127(9):1953-60.
835 44. Suster ML, Abe G, Schouw A, Kawakami K. Transposon-mediated BAC transgenesis in
836 zebrafish. Nat Protoc. 2011;6(12):1998-2021.
837 45. Huang CJ, Tu CT, Hsiao CD, Hsieh FJ, Tsai HJ. Germ-line transmission of a
838 myocardium-specific GFP transgene reveals critical regulatory elements in the cardiac myosin
839 light chain 2 promoter of zebrafish. Dev Dyn. 2003;228(1):30-40.
840 46. Warming S, Costantino N, Court DL, Jenkins NA, Copeland NG. Simple and highly
841 efficient BAC recombineering using galK selection. Nucleic Acids Res. 2005;33(4):e36.
842 47. Bindels DS, Haarbosch L, van Weeren L, Postma M, Wiese KE, Mastop M, et al.
843 mScarlet: a bright monomeric red fluorescent protein for cellular imaging. Nat Methods.
844 2017;14(1):53-6.
845 48. Morawska M, Ulrich HD. An expanded tool kit for the auxin-inducible degron system in
846 budding yeast. Yeast. 2013;30(9):341-51.

847 49. Zhang L, Ward JD, Cheng Z, Dernburg AF. The auxin-inducible degradation (AID)
848 system enables versatile conditional protein depletion in C. elegans. Development.
849 2015;142(24):4374-84.
850 50. Thisse C, Thisse B. High-resolution in situ hybridization to whole-mount zebrafish
851 embryos. Nat Protoc. 2008;3(1):59-69.
852
853

## Figures and Figure legends

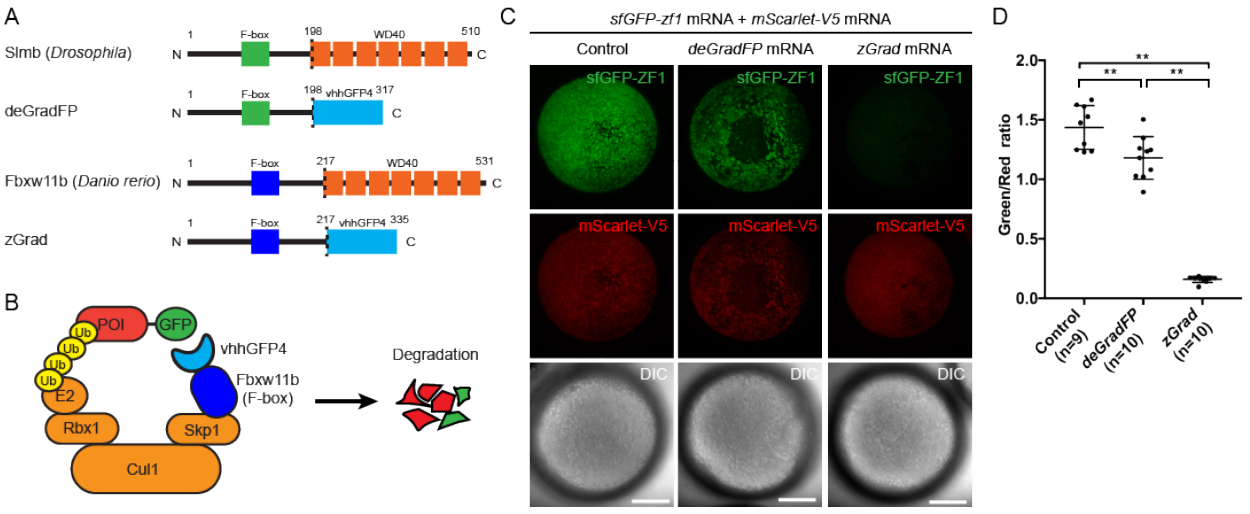


**Figure 1: zGrad degrades GFP-tagged proteins in zebrafish**

(A) Comparison of deGradFP and zGrad fusion proteins.

(B) Schematic of zGrad-mediated target protein degradation. POI: protein of interest.

(C) Representative images of embryos injected with sfGFP-ZF1 mRNA and mScarlet-V5 mRNA (left column) or with sfGFP-ZF1 mRNA and mScarlet-V5 mRNA and deGradFP mRNA (middle column) or zGrad mRNA (right column). Note that mScarlet-V5 fluorescence served as an internal control. Scale bar: 200 μm. ** $p<0.01$.

(D) Quantification of control, deGradFP-mediated and zGrad-mediated sfGFP-ZF1 degradation shown in C.

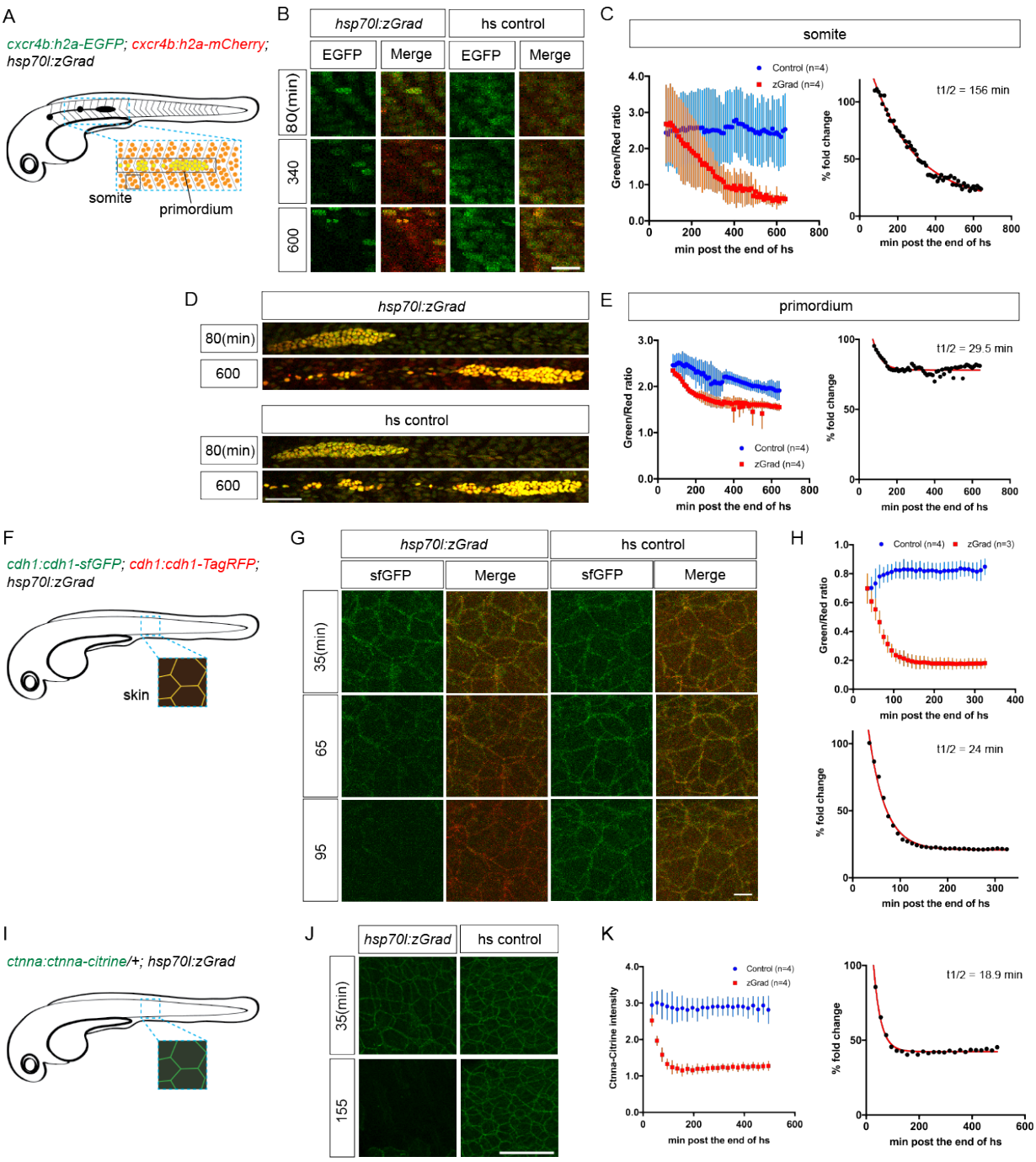


**Figure 2: zGrad degrades nuclear, transmembrane and cytoplasmic proteins**

(A) Schematic of strategy to assess zGrad-mediated H2A-EGFP degradation in the somites and the primordium.

(B) Maximum-projected confocal images of somatic nuclei in heat-shocked *cxcr4b:H2A-EGFP*; *cxcr4b:H2A-mCherry* embryos transgenic for *hsp70l:zGrad* (left) or not (right) at indicated time in min after the end of heat shock (29-30 hpf). Scale bar: 20 µm.

(C) Left, quantification of H2A-EGFP-to-H2A-mCherry ratios in the somites of control (blue) and zGrad-expressing embryos (red) after the end of heat shock in min. Mean and SD are indicated. Right, H2A-EGFP-to-H2A-mCherry ratio of zGrad-expressing embryos normalized to control embryos (black dots) and fitted to a one-exponential decay model (red).

(D) Maximum-projected confocal images of primordium nuclei in heat-shocked *cxcr4b:H2A-EGFP*; *cxcr4b:H2A-mCherry* embryos transgenic for *hsp70l:zGrad* (top) or not (bottom) at indicated time in min after the end of heat shock (29-30 hpf). Scale bar: 50 µm.

(E) Left, quantification of H2A-EGFP-to-H2A-mCherry ratios in the primordia of control (blue) and zGrad-expressing embryos (red) after the end of heat shock in min. Mean and SD are indicated. Right, H2A-EGFP-to-H2A-mCherry ratio of zGrad-expressing embryos normalized to control embryos (black dots) and fit to a one-exponential decay model (red).

(F) Schematic of strategy to assess zGrad-mediated Cdh1-sfGFP degradation in the skin (enveloping and epidermal basal layer).

(G) Maximum-projected confocal images of the skin in heat-shocked *cdh1:cdh1-sfGFP*; *cdh1:cdh1-TagRFP* embryos transgenic for *hsp70l:zGrad* (left) or not (right) at indicated time in min after the end of heat shock (31 hpf). Scale bar: 10 µm.

(H) Top, quantification of Cdh1-sfGFP-to-Cdh1-TagRFP ratios in the primordia of control (blue) and zGrad-expressing embryos (red) after the end of heat shock in min. Mean and SD are indicated. Bottom, Cdh1-sfGFP-to-Cdh1-TagRFP ratio of zGrad-expressing embryos normalized to control embryos (black dots) and fit to a one-exponential decay model (red).

(I) Schematic of strategy to assess zGrad-mediated Ctnna-Citrine degradation in the skin.

898 (J) Maximum-projected confocal images of skin cells in heat-shocked *ctnna:ctnna-Citrine*
899 embryos transgenic for *hsp70l:zGrad* (left) or non-*hsp70l:zGrad* transgenic controls (right) at
900 indicated time in min past the end of heat shock (31 hpf). Scale bar: 50 μm.
901 (K) Left, quantification of Ctnna-Citrine levels in the skin of control (blue) and zGrad-expressing
902 embryos (red) after the end of heat shock in min. Mean and SD are indicated. Right, Ctnna-
903 Citrine levels in zGrad-expressing embryos normalized to Ctnna-Citrine levels in control
904 embryos (black dots) and fit to a one-exponential decay model (red).
905

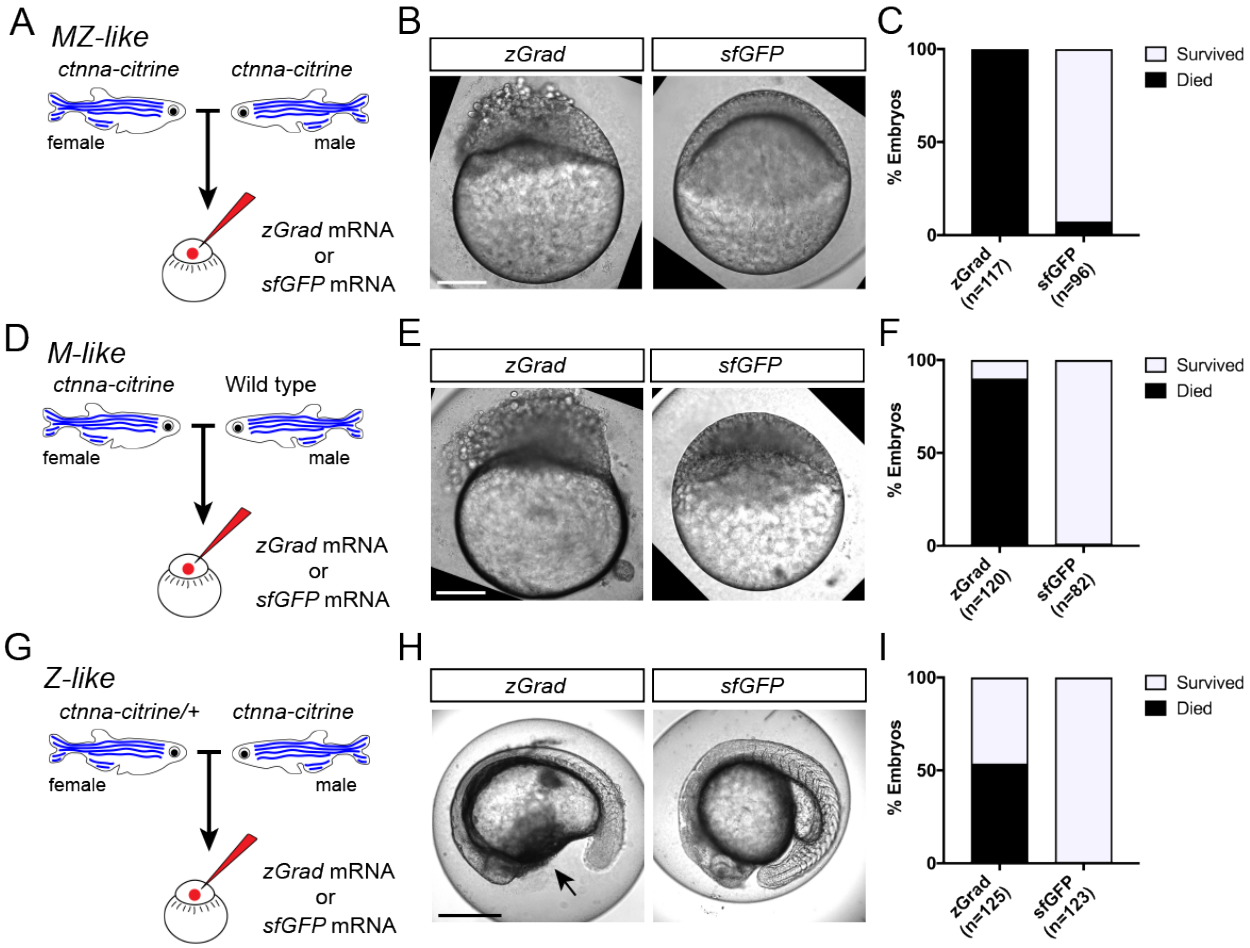


**Figure 3: zGrad-mediated depletion of alpha-Catenin results in cell adhesion defects**

(A) Breeding strategy to assess zGrad-mediated degradation of maternally and zygotically provided Ctnna-Citrine on embryonic development.

(B) Images of MZ *ctnna:ctnna-Citrine* embryos injected with *zGrad* mRNA or *sfGFP* mRNA. Scale bar: 100 µm.

(C) Quantification of MZ *ctnna:ctnna-Citrine* embryos injected with *zGrad* mRNA or *sfGFP* mRNA that disintegrated and died.

(D) Breeding strategy to assess zGrad-mediated degradation of maternally provided Ctnna-Citrine on embryonic development.

(E) Images of M *ctnna:ctnna-Citrine* embryos injected with *zGrad* mRNA or *sfGFP* mRNA. Scale bar: 100 µm.

(F) Quantification of M *ctnna:ctnna-Citrine* embryos injected with *zGrad* mRNA or *sfGFP* mRNA that disintegrated and died.

(G) Breeding strategy to assess zGrad-mediated degradation of zygotically provided Ctnna-Citrine on embryonic development.

(H) Images of Z *ctnna:ctnna-Citrine* embryos injected with *zGrad* mRNA or *sfGFP* mRNA. Scale bar: 100 µm.

(I) Quantification of Z *ctnna:ctnna-Citrine* embryos injected with *zGrad* mRNA or *sfGFP* mRNA that displayed tissue rupture (arrow) and died.

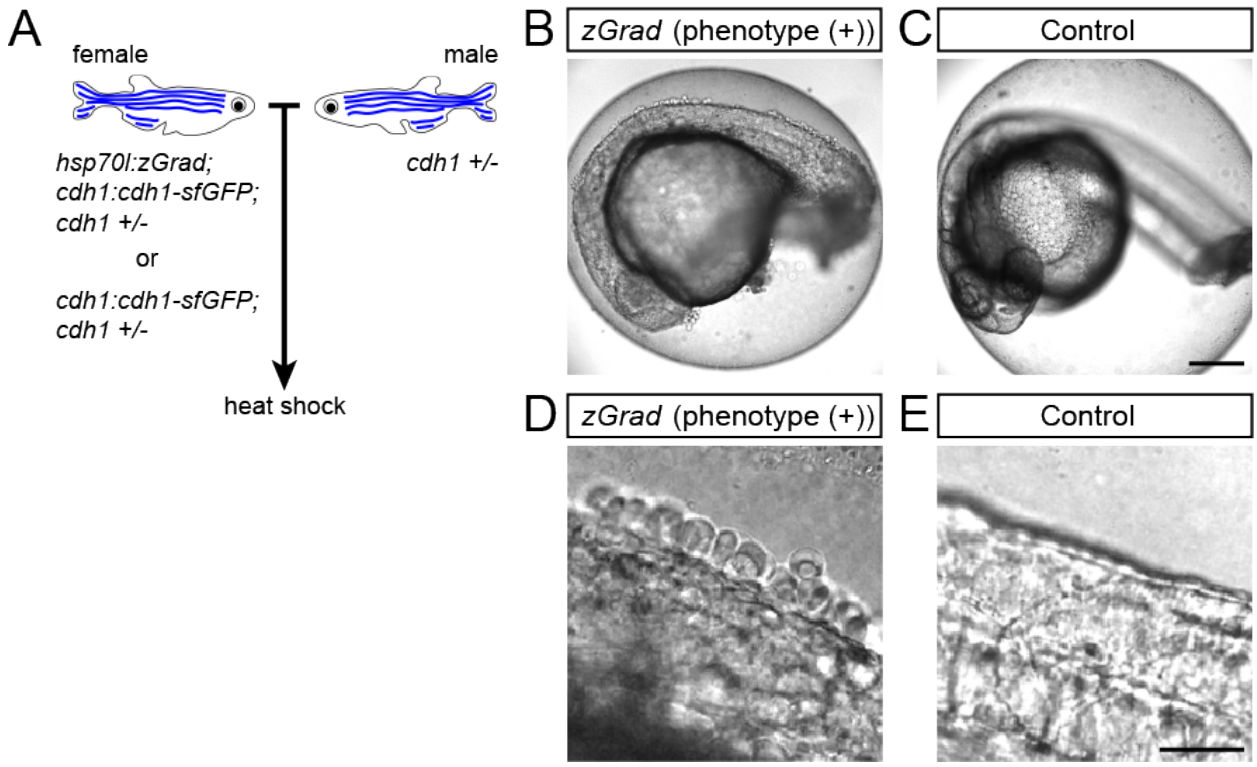


928

929

930 **Figure 4: zGrad-mediated depletion of Cadherin-1 at 25 hpf results in skin defects and**

931 **lethality**

932 (A) Breeding strategy to assess heat shock-induced zGrad degradation of Cdh1-sfGFP on

933 embryonic development.

934 (B, C) Images of *cdh1:cdh1-sfGFP* embryo with skin defects (B) and control embryo (C) at 29

935 hpf. Embryos were heat shocked at 25 hpf for one hour. Scale bar: 200 µm.

936 (D, E) Images of the dorsal trunk of *cdh1:cdh1-sfGFP* embryo with skin cells detaching (D) and

937 control embryo (E) at 29 hpf. Embryos were heat shocked at 25 hpf for one hour. Scale bar: 50

938 µm.

939

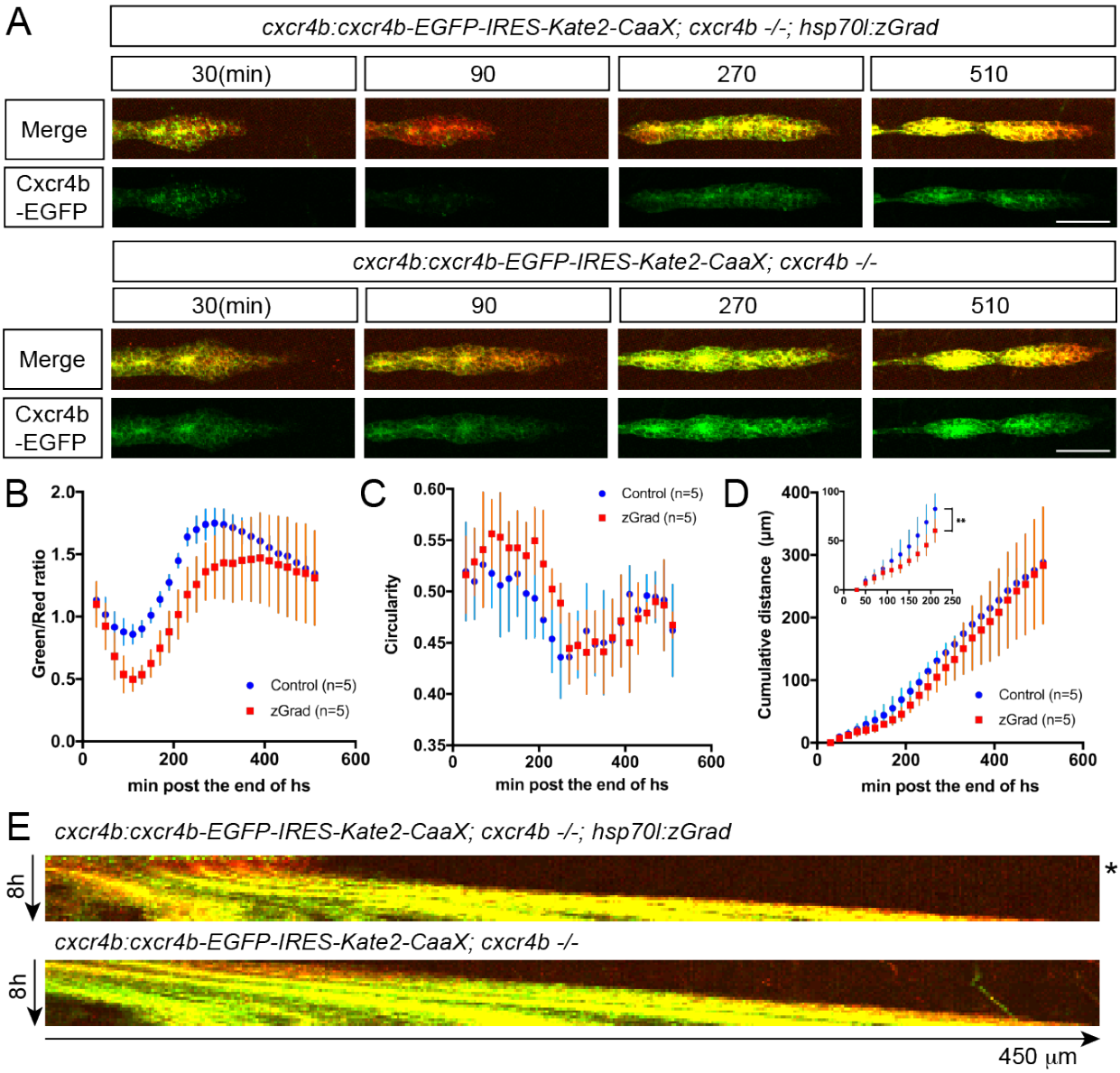


**Figure 5: A pulse of zGrad degrades Cxcr4b-GFP and stalls primordium migration transiently**

(A) Maximum-projected confocal images of the primordia in heat-shocked *cxcr4b:cxcr4b-EGFP-IRES-Kate2-CaaX-p7*; *cxcr4b-/-* embryos transgenic for *hsp70l:zGrad* (upper panels) or not (lower panels) at indicated time in min after the end of heat shock (31 hpf). Scale bar: 50 μm.

947 (B) Quantification of Cxcr4b-EGFP-to-Kate2-CaaX ratios in the primordia of control (blue) and
948 zGrad-expressing embryos (red) after the end of heat shock in min. Mean and SD are indicated.
949 (C) Quantification of circularity of the primordia of control (blue) and zGrad-expressing embryos
950 (red) after the end of heat shock in min. Mean and SD are indicated.
951 (D) Quantification of the cumulative primordium migration distance in control (blue) and zGrad-
952 expressing embryos (red) after the end of heat shock in min. Mean and SD are indicated. Inset
953 shows magnification of the 30 min to 240 min time interval. ** = $p<0.01$.
954 (E) Kymograph of the primordia in heat-shocked *cxcr4b:cxcr4b-EGFP-IRES-Kate2-CaaX-p7*;
955 *cxcr4b-/-* embryos transgenic for *hsp70l:zGrad* (top) or not (bottom). Cxcr4b-EGFP is shown in
956 green and Kate2-CaaX in red. Asterisk indicates the time interval in which Cxcr4b-EGFP is
957 transiently degraded and the primordium transiently ceases to migrate.
958

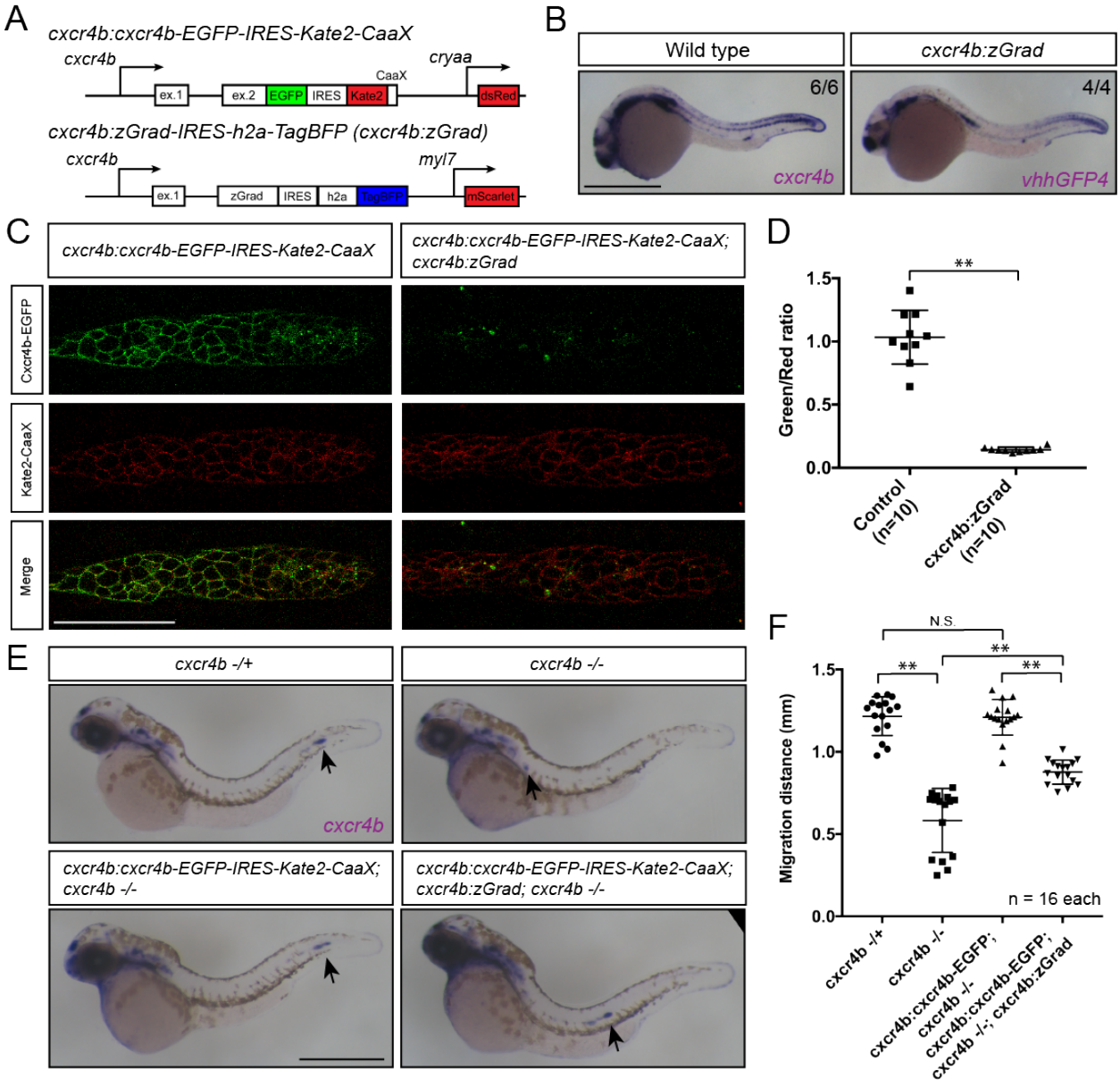


**Figure 6: Tissue-specific expression of zGrad in the primordium degrades Cxcr4b-EGFP and slows down primordium migration**

(A) Schematic of strategy to assess zGrad-mediated Cxcr4b-EGFP degradation in the primordium on primordium migration.

(B) *In situ* hybridization against *cxcr4b* mRNA in a wildtype embryo and against *zGrad* mRNA in a *cxcr4b:zGrad* embryo at 24hpf. Scale bar: 0.5 mm.

967 (C) Single-plane confocal images of the primordium in *cxcr4b:cxcr4b-EGFP-IRES-Kate2-CaaX-*
968 *p1* control (left) and *cxcr4b:cxcr4b-EGFP-IRES-Kate2-CaaX-p1; cxcr4b:zGrad* embryos (right)
969 at 36 hpf. Note that the embryos are *cxcr4b* +/- or *cxcr4b -/-*. Scale bar: 50 μm.
970 (D) Quantification of Cxcr4b-EGFP to Kate2-CaaX fluorescence intensity ratio in the primordia
971 of control embryos (blue) and embryos expressing zGrad in the primordium at 36 hpf. Mean and
972 SD are indicated. ** = $p<0.01$.
973 (E) *In situ* hybridization against *cxcr4b* mRNA in *cxcr4b*-/+ (top left), *cxcr4b*-/- (top right),
974 *cxcr4b:cxcr4b-EGFP-IRES-Kate2-CaaX-p1; cxcr4b-/-* (bottom left) and *cxcr4b:cxcr4b-EGFP-*
975 *IRES-Kate2-CaaX-p1; cxcr4b-/-; cxcr4b:zGrad* embryos (bottom right) at 38 hpf. Arrows indicate
976 the location of the primordium. Scale bar: 0.5 mm.
977 (F) Quantification of primordia migration distance of the indicated genotypes at 38 hpf. Mean,
978 SD and n are indicated. ** = $p<0.01$, N.S. = $p>0.05$.
979

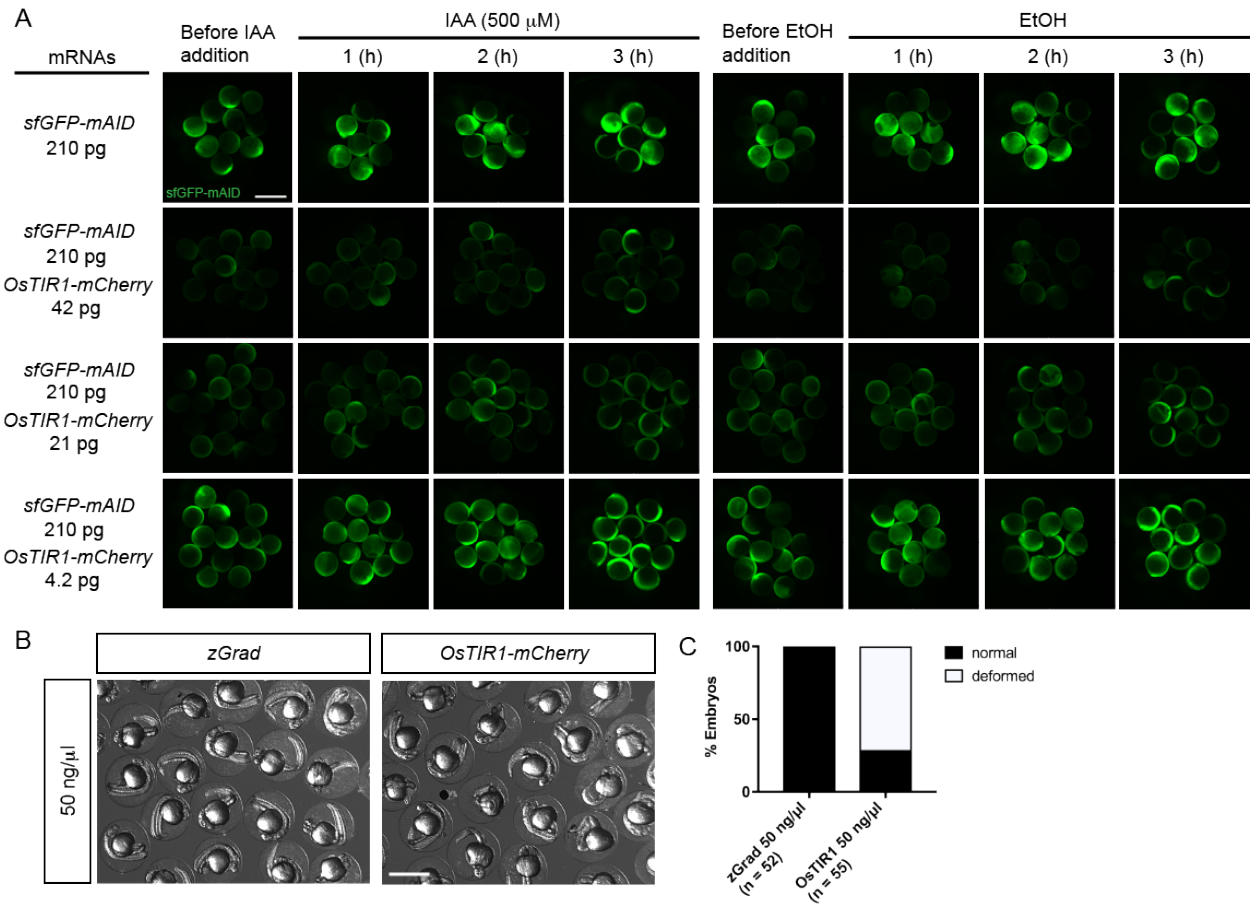


**Figure 1 – figure supplements 1: Characterization of the AID system in zebrafish**

(A) Images of embryos injected with *sfGFP-mAID* mRNA and different amounts of *OsTIR1-mCherry* mRNA and incubated with the auxin IAA (left) or 0.2%EtOH (right) over a 3 hour time course. Scale bar: 1 mm.

(B) Images of embryos injected with *zGrad* mRNA and *OsTIR1-mCherry* mRNA at 24 hpf. Scale bar: 1 mm.

(C) Percentage of deformed embryos among embryos injected with *zGrad* mRNA and *OsTIR1-mCherry* mRNA at 24 hpf.

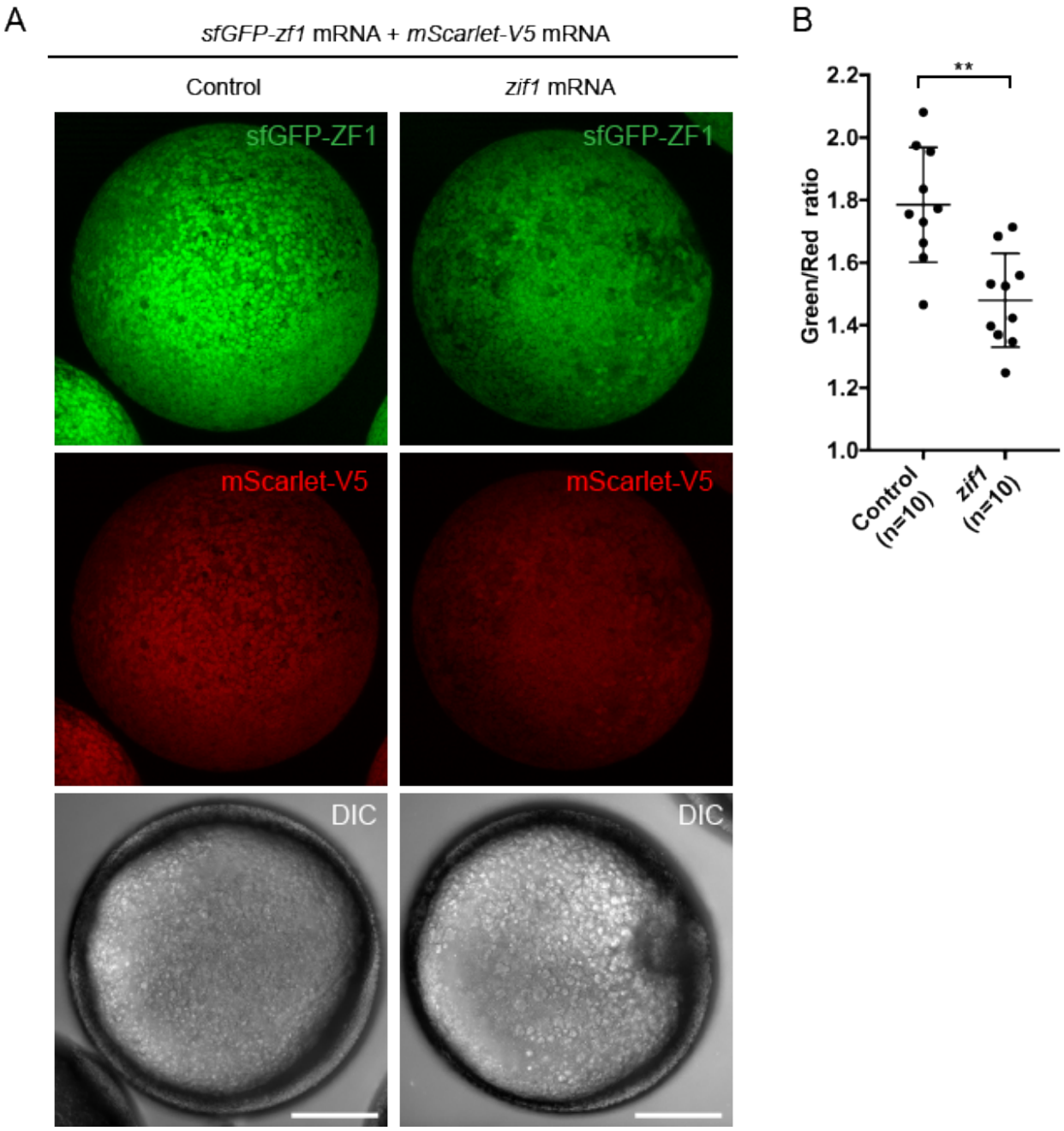


991

992

993 **Figure 1 – figure supplements 2: Characterization of the ZIF1 system in zebrafish**

994 (A) Images of embryos injected with *sfGFP-zf1* mRNA and *mScarlet-V5* mRNA (left) and

995 embryos injected with *sfGFP-zf1* mRNA, *mScarlet-V5* mRNA and *zif1* mRNA (right) at 6 hpf.

996 Scale bar: 200 μm.

997 (B) Quantification of the sfGFP-to-mScarlet fluorescence intensity ratio in the embryos shown in

998 A. Mean, SD and n are indicated. ** = $p<0.01$.

999

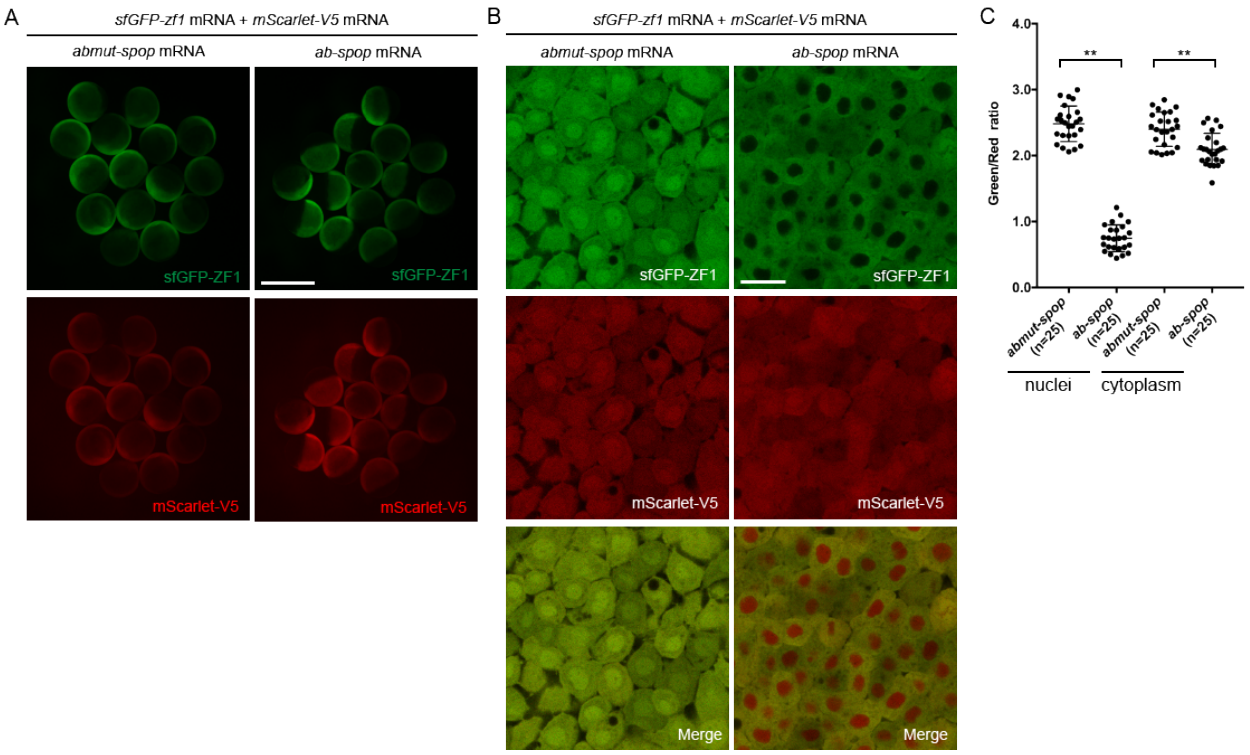


**Figure 1 – figure supplements 3: Characterization of the Ab-SPOP system in zebrafish**

(A) Images of embryos injected with *sfGFP-zf1* mRNA, *mScarlet-V5* mRNA and *abmut-spop* mRNA (left in A) or *ab-spop* mRNA (right in A) at 6 hpf. Scale bar: 1 mm.

(B) Single-plane confocal images of cells in embryos injected with *sfGFP-zf1* mRNA, *mScarlet-V5* mRNA and *abmut-spop* mRNA (left in A) or *ab-spop* mRNA (right in A) at 6 hpf. Scale bar: 20 μm.

(C) Quantification of the sfGFP-to-mScarlet fluorescence intensity ratio in the nuclei and the cytoplasm of embryos shown in B. Mean, SD and n are indicated. ** = $p<0.01$.

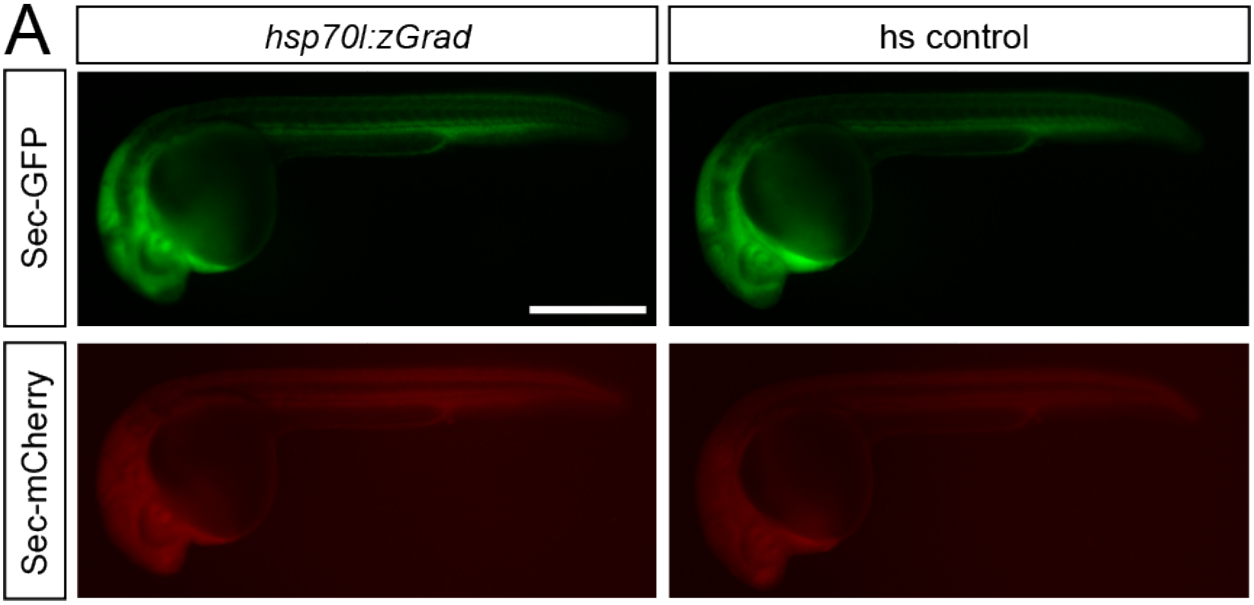


**Figure 2 – figure supplement 1: zGrad does not degrade secreted proteins**

(A) Images of *hsp70l:sec-GFP*; *hsp70:sec-mCherry*; *hsp70l:zGrad* embryos (left) and *hsp70:sec-GFP*; *hsp70:sec-mCherry* control embryos (right) 5 hours post heat-shock at 30 hpf. Scale bar: 50 μm.

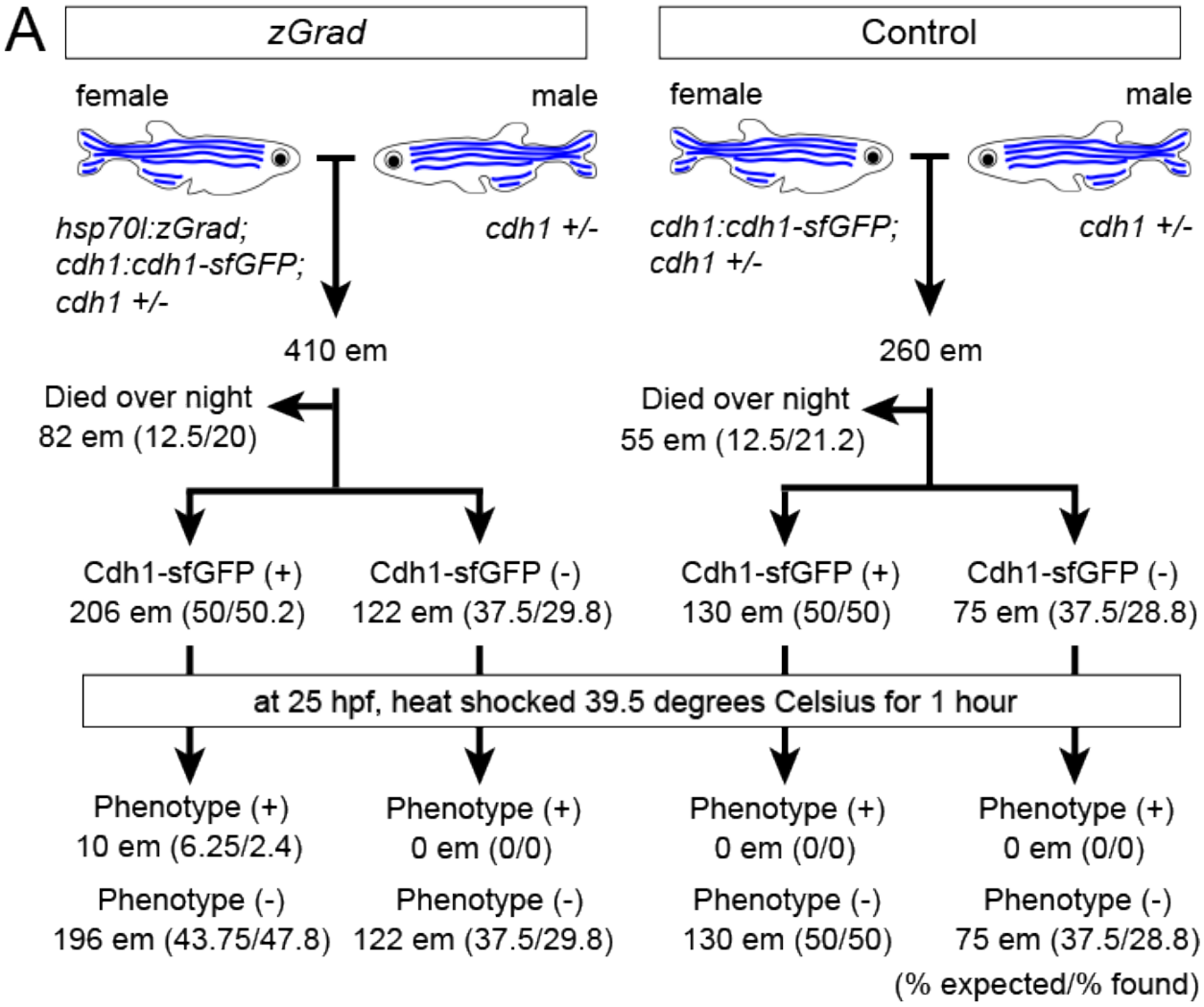


**Figure 4 – figure supplement 1: Expected results for zGrad-induced depletion of sfGFP-tagged Cadherin-1**

(A) Crossing scheme of indicated genotypes and % of embryos with expected and observed phenotype.

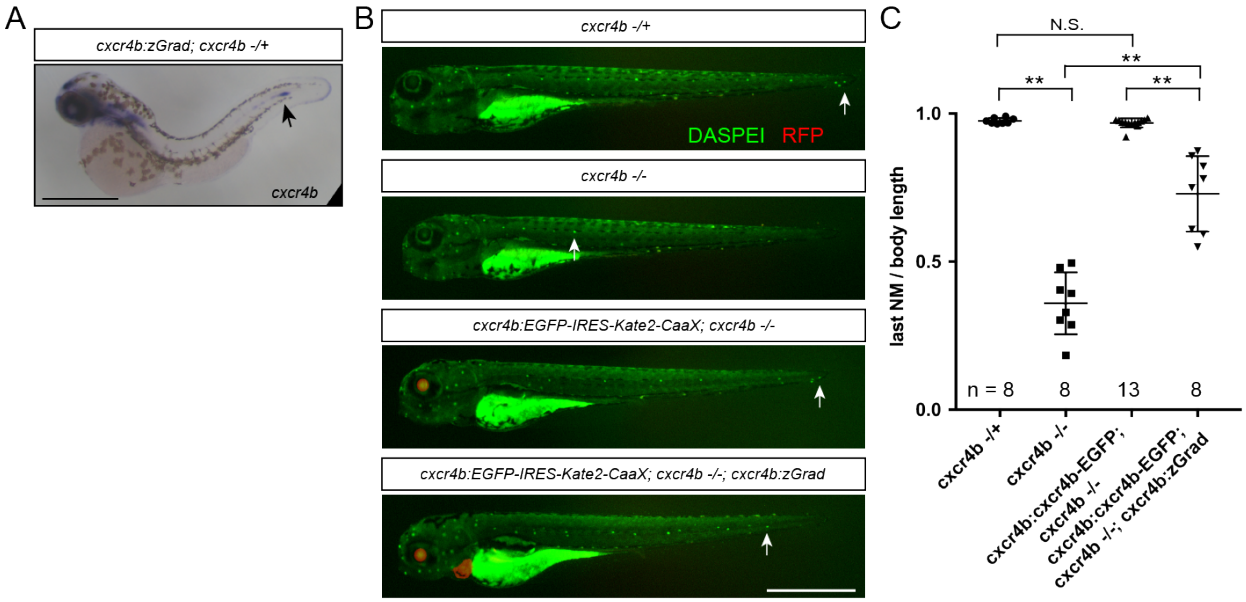


**Figure 6 – figure supplement 1: Tissue-specific Cxcr4b-EGFP degradation by zGrad**

(A) *In situ* hybridization against *cxcr4b* mRNA in a 38 hpf *cxcr4b:zGrad; cxcr4b -/+* embryo. Arrow indicates the location of the primordium. Scale bar: 0.5 mm.

(B) Images of live embryos of indicated genotypes stained for neuromasts with DASPEI at 4 dpf. Note that the *cxcr4b:cxcr4b-EGFP-IRES-Kate2-CaaX-p1* transgene carries *cryaa:dsRed*, which expresses dsRED in the lens, and the *cxcr4b:zGrad* transgene carries *cmlc2:mScarlet*, which expresses mScarlet in the myocardium, as transgenic markers. Arrows indicate the position of the last neuromast. Scale bar: 1 mm.

(C) Quantification of the position of the last neuromast normalized to body length of embryos shown in B. ** = $p<0.01$, N.S. = $p>0.05$.

**Table 1: *Cdh1* transgenic lines rescue *cdh1* mutants**

| Transgenic line | Total number of embryos | Transgenic embryos phenotypically wild type | Non-transgenic embryos phenotypically wild type | Embryos phenotypically *cdh1* mutant |
|---|---|---|---|---|
| *cdh1:cdh1-sfGFP* | 306 (100 %) | 149 (47 %) | 96 (33 %) | 61 (20 %) |
| *cdh1:cdh1-TagRFP* | 432 (100 %) | 204 (47 %) | 172 (40 %) | 56 (13%) |

**Table 2: Summary of degradation kinetics**

| FP-Tagged protein | Promoter expressing zGrad | Percent reduction | Degradation half-life in min | time for onset of degradation in min |
|---|---|---|---|---|
| sfGFP-ZF1 | mRNA | 89 % | N/A | N/A |
| Cxcr4b-EGFP | *cxcr4b* | 86 % | N/A | N/A |
| H2A-EGFP (in somites) | *hsp70l* | 87 % | 156 | 200 |
| H2A-EGFP (in primordium) | *hsp70l* | 22 % | *29** | 140 |
| Cdh1-sfGFP | *hsp70l* | 79 % | 24 | 75 |
| Ctnna-Citrine | *hsp70l* | 58 % | 19 | 65 |

* Note that the zGrad-mediated degradation of H2A-EGFP in the primordium is obscured by the continued production of H2A-EGFP.

**Figure 2 – Video 1: Degradation of H2A-EGFP by zGrad expressed from *hsp70l* promoter**

Heat-shocked *hsp70l:zGrad; cxcr4b:h2a-EGFP; cxcr4b:h2a-mCherry* embryo (top) and heat-shocked *cxcr4b:h2a-EGFP; cxcr4b:h2a-mCherry* control embryo (bottom). Time stamp indicates min after the end of the heat shock. Images are maximum-projected. Green: H2A-EGFP, Red: H2A-mCherry. Scale bar corresponds to 50 μm.

**Figure 2 – Video 2: Degradation of Cdh1-sfGFP by zGrad expressed from *hsp70l* promoter**

Heat-shocked *hsp70l:zGrad; cdh1:cdh1-sfGFP; cdh1:cdh1-TagRFP* embryo (left) and heat-shocked *cdh1:cdh1-sfGFP; cdh1:cdh1-TagRFP* control embryo (right). Time stamp indicates min after the end of the heat shock. Images are maximum-projected. Green: Cdh1-sfGFP, Red: Cdh1-TagRFP. Scale bar corresponds to 10 μm.

**Figure 2 – Video 3: Degradation of Ctnna-Citrine by zGrad expressed from *hsp70l* promoter**

Heat-shocked *hsp70l:zGrad; ctnna:ctnna-citrine/+* embryo (left) and heat-shocked *ctnna:ctnna-citrine/+* control embryo (Right). Time stamp indicates min after the end of the heat shock. Images are maximum-projected. Green: Ctnna-Citrine. Scale bar corresponds to 10 μm.

**Figure 5 – Video 1: Degradation of Cxcr4b-EGFP by zGrad expressed from *hsp70l* promoter**

Heat-shocked *hsp70l:zGrad; cxcr4b:cxcr4b-EGFP-IRES-Kate2-CaaX-p1; cxcr4b -/-* embryo (top) and heat-shocked *cxcr4b:cxcr4b-EGFP-IRES-Kate2-CaaX-p1; cxcr4b -/-* control embryo (Bottom). Time stamp indicates min after the end of the heat shock. Images are maximum-projected. Green: Cxcr4b-EGFP, Red: Kate2-CaaX. Scale bar corresponds to 50 μm.